UNIVERSITY OF WEST BOHEMIA
FACULTY OF MECHANICAL ENGINEERING

Study Program: N2301 Mechanical Engineering
Field of Study: Design of Power Machines and Equipment

MASTER THESIS

Aerodynamic measurements on stationary and vibrating turbine blade cascade

Autor: **Izzat KASS HANNA**

Vedoucí práce: **Doc. Ing. Petr ERET, Ph.D.**

Academic year 2018/2019

ZÁPADOČESKÁ UNIVERZITA V PLZNI
Fakulta strojní
Akademický rok: **2018/2019**

ZADÁNÍ DIPLOMOVÉ PRÁCE

(PROJEKTU, UMĚLECKÉHO DÍLA, UMĚLECKÉHO VÝKONU)

Jméno a příjmení:	**Izzat KASS HANNA**
Osobní číslo:	**S16N0043P**
Studijní program:	**N2301 Strojní inženýrství**
Studijní obor:	**Stavba energetických strojů a zařízení**
Název tématu:	**Aerodynamic measurements on stationary and vibrating turbine blade cascade**
Zadávající katedra:	**Katedra energetických strojů a zařízení**

Zásady pro vypracování:

1. Overview of turbine blade cascade testing (pressure profiles, flutter).
2. Experimental setup and measurement techniques.
3. Testing on stationary and vibrating blade cascade and data analysis.

Skills:

- Vibrations, Fluid mechanics, Wind tunnel testing.
- English language.

Rozsah grafických prací: -

Rozsah kvalifikační práce: **50 - 70 stran**

Forma zpracování diplomové práce: **tištěná/elektronická**

Jazyk zpracování diplomové práce: **Angličtina**

Seznam odborné literatury:

- **Slama V., Rudas B., Ira J., Macalka A., Eret P., Tsymbalyuk V.: CFD prediction of flutter of turbine blades and comparison with an experimental test case, 2018, MATEC Web of Conferences 168, 2005**
- **Tsimbalyuk V. A.: Method of measuring transient aerodynamic forces and moments on a vibrating cascade, Strength Mater (1996) 28: 150**
- **Vogt D., 2005: Experimental Investigation of Three-Dimensional Mechanisms in Low-Pressure Turbine Flutter, KTH, PhD thesis**
- **Nowinski M., Panovsky J., 1999: Flutter Mechanisms in Low Pressure Turbine Blades, Eng J.: Gas Turbines Power 122 (1), 82-88**

Vedoucí diplomové práce: **Doc. Ing. Petr Eret, Ph.D.**
Katedra energetických strojů a zařízení

Konzultant diplomové práce: **Doc. Ing. Petr Eret, Ph.D.**
Katedra energetických strojů a zařízení

Datum zadání diplomové práce: **30. října 2018**

Termín odevzdání diplomové práce: **24. května 2019**

Doc. Ing. Milan Edl, Ph.D.
děkan

L.S.

Dr. Ing. Jaroslav Synáč
vedoucí katedry

V Plzni dne 25. října 2018

Declaration

I hereby declare that this master thesis is entirely my own work and that I only used the cited sources.

V Plzni dne: . . . . . .

Acknowledgement

I would like to express my very profound gratitude to my supervisor, Petr Eret for the useful comments, remarks and engagement from the beginning to the very end of my master thesis. I truly appreciate his helpful advice and generous help.

Furthermore, my deepest and sincere gratitude goes to my family for their unflagging and unparalleled love, help and support throughout my life and my studies.

ANOTAČNÍ LIST DIPLOMOVÉ PRÁCE

AUTOR	**Příjmení** Kass Hanna	**Jméno** Izzat	
STUDIJNÍ OBOR	ESZN „ Stavba energetických strojů a zařízení “		
VEDOUCÍ PRÁCE	**Příjmení (včetně titulů)** Doc. Ing. Eret, Ph.D.	**Jméno** Petr	
PRACOVIŠTĚ	ZČU - FST - KKE		
DRUH PRÁCE	**DIPLOMOVÁ**	~~**BAKALÁŘSKÁ**~~	**Nehodící se škrtněte**
NÁZEV PRÁCE	Aerodynamic measurements on stationary and vibrating turbine blade cascade		

FAKULTA	strojní		**KATEDRA**	KKE	**ROK ODEVZD.**	2019

POČET STRAN (A4 a ekvivalentů A4)

CELKEM	58	**TEXTOVÁ ČÁST**	50	**GRAFICKÁ ČÁST**	0

STRUČNÝ POPIS (MAX 10 ŘÁDEK) **ZAMĚŘENÍ, TÉMA, CÍL POZNATKY A PŘÍNOSY**	Diplomová práce obsahuje experimentalní studium lopatkové mříže a tlakové ztraty na ruzních uhely naběhu a vyšky .
KLÍČOVÁ SLOVA **ZPRAVIDLA JEDNOSLOVNÉ POJMY, KTERÉ VYSTIHUJÍ PODSTATU PRÁCE**	Lopatkové mříže, Vibrace, Flutter, Turbínové lopatký, aerodynamicky veličiny. Mechanika tekutin

SUMMARY OF DIPLOMA SHEET

AUTHOR	**Surname** Kass Hanna	**Name** Izzat	
FIELD OF STUDY	ESZN "Department of Power System Engineering "		
SUPERVISOR	**Surname (Inclusive of Degrees)** Doc. Ing. Eret, Ph.D.	**Name** Petr	
INSTITUTION	ZČU - FST - KKE		
TYPE OF WORK	**DIPLOMA**	~~**BACHELOR**~~	**Delete when not applicable**
TITLE OF THE WORK	Aerodynamic measurements on stationary and vibrating turbine blade cascade		

FACULTY	Mechanical Engineering		**DEPARTMENT**	KKE	**SUBMITTED IN**	2019

NUMBER OF PAGES (A4 and eq. A4)

TOTALLY	60		**TEXT PART**	50	**GRAPHICAL PART**	0

BRIEF DESCRIPTION **TOPIC, GOAL, RESULTS AND CONTRIBUTIONS**	This thesis dissert on experimental study for aerodynamic forces and pressure lost measured in a linear blade cascade, oscillating phenomenon.
KEY WORDS	Turbine blade cascade, Aerodynamic forces and moments, experiment, test rig, linear cascade, vibration, fluid mechanics

Table of Contents

Tables of Figures

Table of Tables

List of Abbreviations

Acronym	Definition
AoA	Angle of Attack
IBPA	Interblade Phase Angle
2D	Two-dimensional
3D	Three-dimensional
deg	Degree
CFD	Computational Fluid Dynamics
ND	Nodal Diameter
CRF	Compressor Research Facility
Ma	Mach's Number

List of Frequently Used Symbols

Symbol	Unit	Property
C	[mm]	Chord of the blade
h	[mm]	Blade length
V_1	[m/s]	Inlet velocity
V_2	[m/s]	Outer velocity
P_o	[Pa]	Static pressure
α1 , α2	[-]	Inlet and outlet angles
ε	[-]	Curvature of the flow
S	[mm]	Pitch
ρ	[kg/m^3]	Density
M	[N.m]	Moment
L	[N]	Lift force
p_c	[Pa]	Total Pressure
p_s	[Pa]	Static pressure
y_n	[mm]	amplitude of bending vibration
a_n	[mm]	amplitude of torsion vibration
P_d, q	[-]	Dynamic pressure
Ma	[-]	Mach's number
W	[J]	aerodynamic work
C_{ps},C_{pc}	[-]	Pressure ratios
t	[^{o}C]	temperature
m_{out}	[kg/s]	Mass flow
C_W	[-]	non-stationary aerodynamic loads coefficient

1 Introduction

In all blade rotating machines, for example hydraulic, steam or gas turbines, compressors, pumps, etc., blades are essential elements. They play an important role along with other machine's parts to convert the power held by the medium into a rotating kinetic power. It can also convert the rotating power given by motor and transfer it to the medium (compressor case). These blades are assembled in a row that creates a wheel. Each stage is made from two blade wheels, fixed and moving wheels.

As the blades are exposed to fluid flow such as water, steam or gas, different temperatures and pressures; this means that they are exposed to aerodynamic, structural forces and moments, also material forces. That makes the topic of blade stability and the effects of fluid is an important topic, due to its big effect on the efficiency of the blade and the turbomachine, its role, ageing and its material properties (strain, fatigue, etc.).

One of the main issues of blades stability is the possibility of a rapid increase of oscillation amplitude. The blade motion is typically damped by the structure, but in some cases, at certain flow velocity, the oscillation of the blade or blade row is induced and grows to a critical level that can cause structural failure or severe damage in the blade structure and material. This is called Flutter and this phenomenon is the topic of this study.

This thesis primarily focuses on an experimental study of the blade cascade stability. However, additional measurements of pressure profiles downstream of the stationary blade cascade were done. A test rig based in the Faculty of Mechanical Engineering, University of West Bohemia was exploited and the tests on the stationary blade cascade were performed for two different Angles of Attack (AoA) and at different positions of the blade height. The flutter measurements on the vibrating blade cascade were carried out only for a single AoA.

This thesis is divided into many parts. First, an overview of blade types and main classifications of blade are presented. Second, a theoretical study of blade cascade types is provided. Third part studies the flutter phenomenon and its reasons, types of oscillations and deformation. The fourth part is an overview of main measurement methods of flutter and a historical review of previous study about it and its results. The fifth part is a description of the test rig, test section, used instruments during experiments. The last part shows the results of different tests performed on a stationary blade cascade, where all the blades are not moving, with AoA equal to 0^o and 5^o. In addition, tests at AoA equal to 0^o were performed at a level 50% of the blade height, while at AoA equal to 5^o in the bottom, middle and at the top of the blade. In the final part of the thesis, flutter tests were performed by oscillating the four central blades in the cascade in a travelling wave mode to measure the aerodynamic work of bending and torsion vibration. The results of all tests were discussed.

1. Classification of blades

Blades in turbomachines differ in profiles, blade length, roots, etc. they have different roles according to their position in the machine and the role of the machine. Which leads to a different classifications of blades. There are many methods of distinguishing the differences between blades, its types and functions, the following methods shows the main sorting of blades:

First methods is according to the position in the turbomachine and the function:

1- Fixed wheels or stator wheels are the wheels connected to the Machine casings, either directly or through a carrier. Its role is to redirect the direction of the flow and speeding it in order to enter the next stage with the best attack angle. Figure 1 shows half of the stator wheel for a turbine.
In stator wheels, the latent energy is transferred to a kinetic energy. For that, the blades profile is built to create a nozzle between the blades and give the best conditions to enter the rotor stage.

2- Moving wheels or the rotor wheels are the blade stages attached to the rotor and move with it. Each moving stage transfers part of the kinetic energy from the medium (Steam, water, gas) into a rotational energy that rotates the rotor. Figure 2 shows an example of two stages rotor.

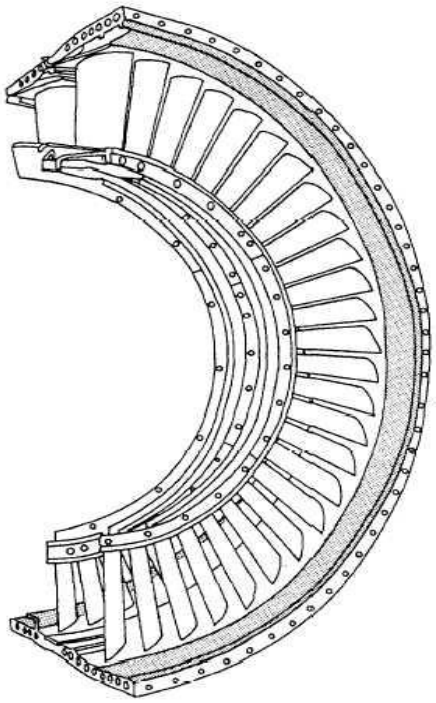

Figure 1 Stator wheel

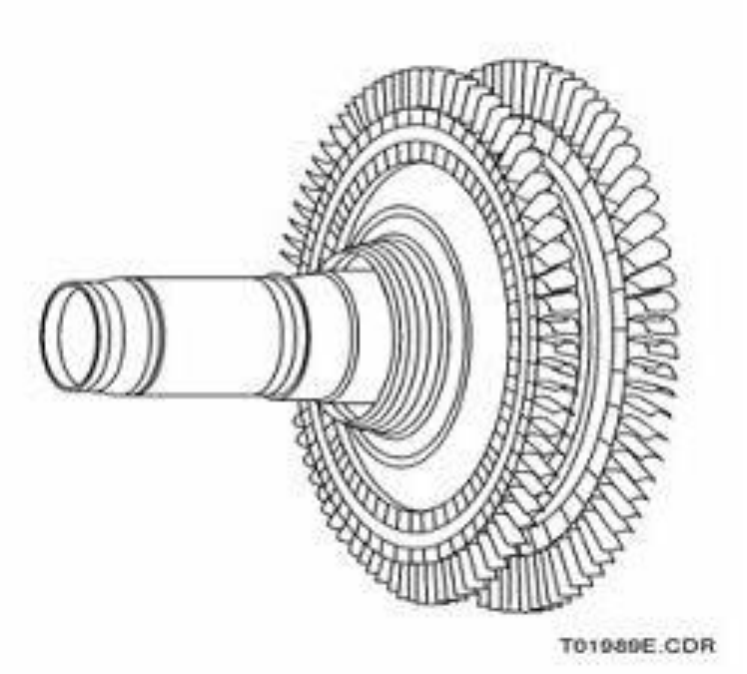

Figure 2 Rotor wheel

Blades can be also by sorted by the direction of flow, thus we can find two types, axial or radial flow. Radial flow can be found in radial compressors, where the flow moves in a radial way away from the rotor. Axial flow is mainly in steam turbines, where the steam goes through stages along with the rotor's axis. Usually in radial flow machines we have only a single stage, and on the other hand, axial flow machines are mostly multi-stages.

Another sorting of Blades can be made according to its function of the machine and here we can find two types:

1- Blades in where the speed of the medium in decreased and the pressure is increased. This type is used in pumps and compressors.

2- Blades in where the medium's speed is increased and the pressure is decreased, as in Turbines.

2. Blade cascade

One of the main problems in the turbine's design is the stability of flow in blades, and especially in the last stages, where the blade length is big and the biggest amount of transferred energy is produced there, so any instability affects the efficiency of the machine.

For this issue, and in order to make the study easier, we can use blade cascade to make the aerodynamic flow less complicated.

Blade cascade is defined as a sector in the blade row at a specific radius, this creates a plane where the pitch between blades is equal, and this plane is unrolled. Figure 3 shows the blade cascade plane and the blade profile after unrolling.

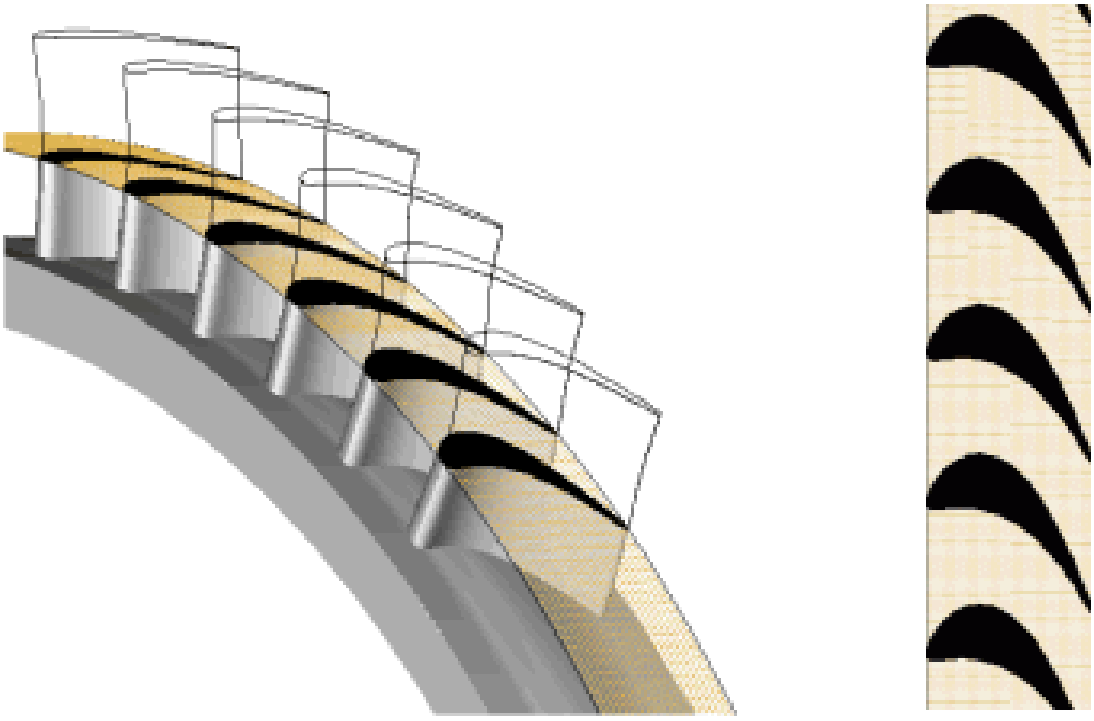

Figure 3 Blade cascade

In order to study it, we should first know the two types of blade cascades. First type is linear cascade, which is made of a row of blades at a given radial section, also this blades are spaced by a pitch that relates to the radius in the actual machine.

The second is annular cascade which is made of a row of blades in the real annular geometry, this cascade is similar to the actual cascade in rotor or stator.

Blade cascade test is an effective way to study the performance of flow and its effects on each blade, it accounts for the geometrical and aerodynamic similarities. Nonetheless, the geometry of the actual blade and the blade section.

Linear cascades provide a 2D flow with a range of non-accuraction, unlike the actual 3D flow in machine. Although this imprecise method do not affect the design of the optimum blade profile and it gives enough details about the flow in the cascade.

3. Geometrical and Aerodynamic parameters of blade cascade

1) Geometrical parameters:

Each blade cascade differs according to the shape of blades and the position of blades in the cascade. For that, the geometrical parameters of blade profiles and cascades are important and play the biggest role in the design process.

Blade profile parameters:

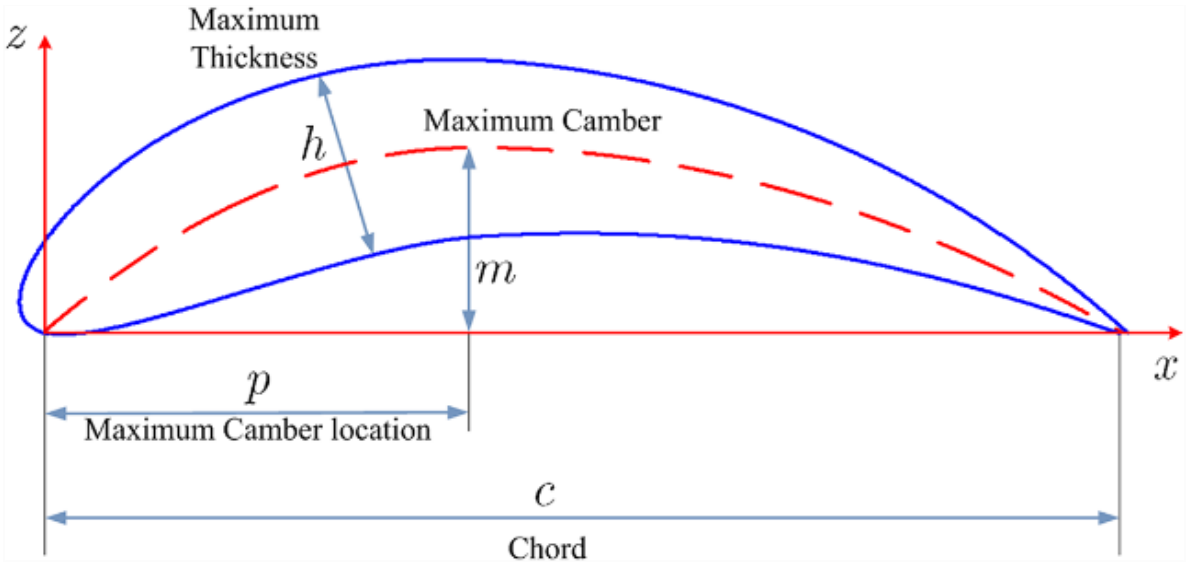

Figure 4 Blade Profile for Turbine Blade

Figure 4 shows the main geometrical parameters for a turbine blade profile, which are:

- Chord of the blade [C],
- maximum thickness of the blade [h],
- p and m are the maximum length and height for Camber line, which is defined as a curved line in which the profile thickness distribution is symmetrically superimposed.

Blade Cascade parameters:

In the turbine blade cascade shown in Figure 5, it is observed the geometrical parameters for the cascade, and they are:

- The pitch of the cascade [S], which is the distance between every two blades and it should be constant along the cascade.

- The S/C ratio, which differs according to the profile or type of cascade, for example for compressors, it is from (0.5 – 2), for impulse turbines is from (0.3 – 0.4), for reaction turbines is from (0.4 – 0.6).

- The angles (θ_1, θ_2, λ, i, δ), where θ_1, θ_2 are the angles between the chord line and the Camber line. λ is stagger angle and δ is the angle between air outlet and Camber line. Changing of λ for the same parameters can lead to even change from Compressor cascade to Turbine cascade.

- The ratio m/C in turbine cascade differs from (0.4 – 0.5)

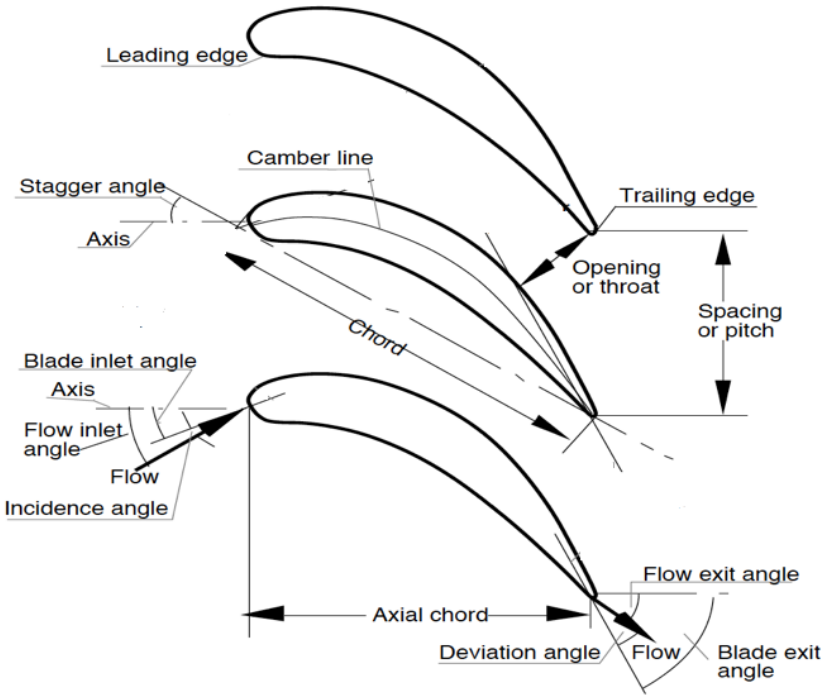

Figure 5 Blade cascade for turbine stator

2) Aerodynamic parameters:

During the flow in blade cascade, some parameters change, which are, the direction of the flow, the velocity of the flow before and after the cascade, the pressure of the flow and the transferred energy, these parameters are aerodynamic parameters, they differ in each blade cascade, and they can be calculated either numerically (CFD) or experimentally.

Figure 6 and 7 show the main aerodynamic parameters, which are:

a. The Vector of inlet and outlet velocities and speed triangles, they are:
   - Inlet velocity V_1 with angles α_1 and ι
   - Outlet velocity V_2 with angles α_2 and δ
   - Curvature of the flow, which is the difference between inlet and outlet angles, it is given by:

$$\varepsilon = \alpha_2 - \alpha_1 \quad (1.1)$$

b. Forces of the flow on the cascade, shown in Figure 7 and also:
   - The average difference of static pressure upstream and downstream cascade P_{01}, P_{02}
   - Spread velocity/ pressure over the profile

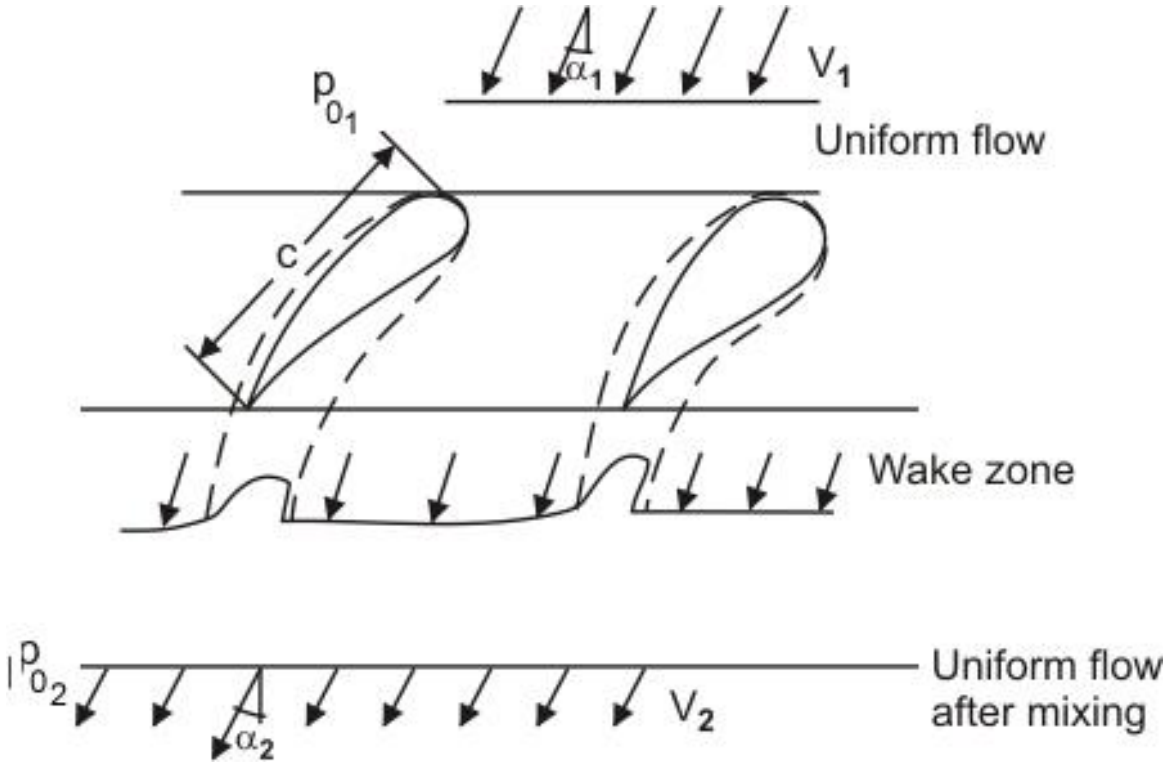

Figure 6 Velocity profile before and after cascade, effect of flow around the blades

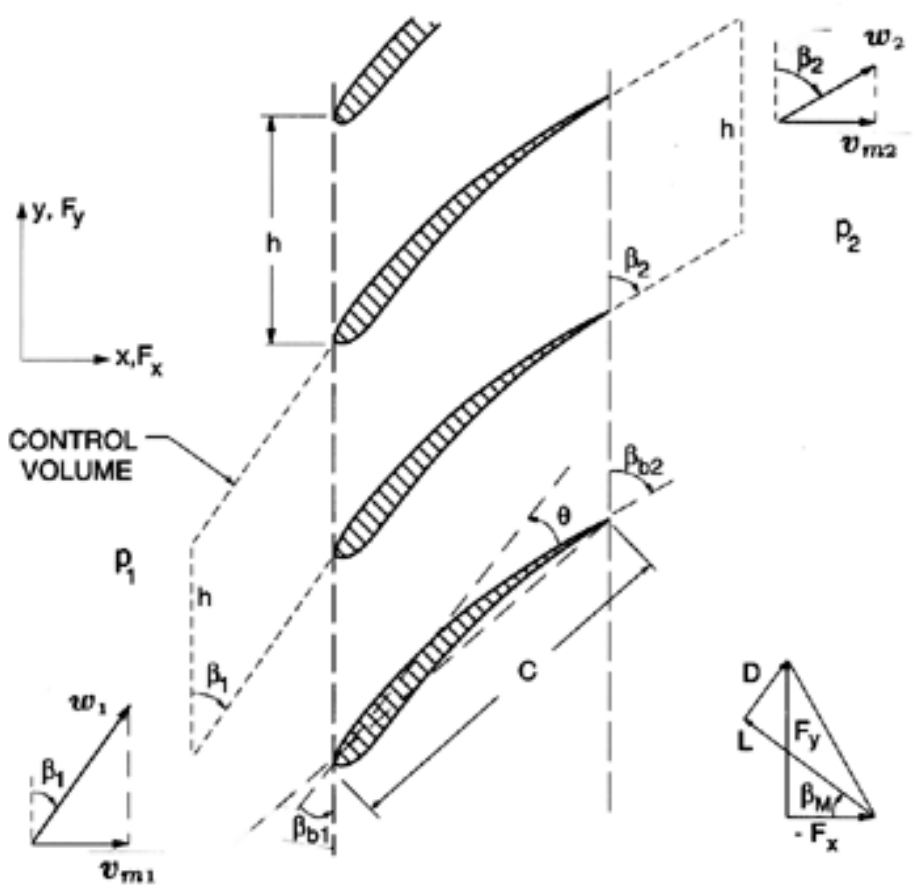

Figure 7 Blade Cascade parameters and forces

Notice in figure 6 that the velocity profile downstream the blade cascade is not constant, and that is due to the separation of the flow around the blades, that affects the stability of the flow.

2 Flutter

1. Description

The most relevant phenomena of aeroelasticity are grouped as follows:

Staticaeroelasticity: balance of steady aerodynamic loads and structural forces. Turbomachinery blades deform during operation due to aerodynamic loads (gas loads) and centrifugal loads. This deformation is mainly of torsional nature (blade untwist). Other types of deformation include changes in profile section (uncamber) and bending. Static aeroelasticity needs to be accounted for when manufacturing blades. Blade geometries at running conditions (often referred to as "hot geometry") need to be calculated back to their shape at rest. This process is referred to as "unrunning" (Marshall and Imregun, 1996).

Forced response: unsteady aerodynamic force due to certain (steady) spatial distribution of flow parameters in one frame of reference that can lead to unsteadiness in another frame of reference. Typical sources of forced response are blade row interaction phenomena or inflow distortion. Forced response is always characterized by deterministic forces that are synchronous to engine rotational speed (Srinivasan, 1997).

Flutter: self-induced vibrations due to initially small unsteadiness which grow rapidly in each oscillation cycle unless properly damped. At a state of flutter the unsteady aerodynamics is feeding energy into the structure leading to rapid escalation of oscillation amplitudes. Flutter can occur in various operating regimes (choke, stall, subsonic, supersonic) and is of primary concern in low-pressure compressor (including fan) and low-pressure turbine components (Srinivasan, 1997). As fan blades are exposed to gusts, cross-winds and foreign object damage (FOD) they are considered more critical with respect to flutter design.

Non-synchronous vibrations (NSV): vibrations, which are not initially induced by motion of blades but rather by inherent flow unsteadiness. Tip leakage flow unsteadiness is one of possible sources for NSV (Thomassin et al. 2007).

Definition of Flutter: is a phenomenon that indicates the vibration of a structure exposed to fluid flow. This vibration causes an instability in the structure, and at certain conditions, it causes small vibrations inside the structure, these vibrations provoke the aerodynamics forces and increase the energy in the body, that leads to a rapidly grow in the magnitude of vibration in each cycle. At this point, it is impossible to prevent the instability and leads to structural damages and material failure.

In Turbomachines, we can distinguish two types of vibrations, resonant vibrations and flutter. In resonant flow, the unsteady flow is not stimulated by the external sources, but by the motion of the body. This unsteadiness leads to structural vibrations. Flutter differs from the first type in the way of stimulation of vibration. In flutter, it is stimulated by the fluid forces on the body, inertial and damping forces and the elastic forces of the structure. All this forces in a specific unstable balance leads to the occurrence of flutter, and it means, that the fluid is inducing the flutter by giving energy to the structure. It leads to rapidly increase of oscillation amplitude with every cycle.

In other word, involvement of Elastic, inertial and aerodynamics forces creates and increases flutter and its effects. Figure 8 shows the Collar's triangle of forces, this shows the phenomenological interaction leading to flutter.

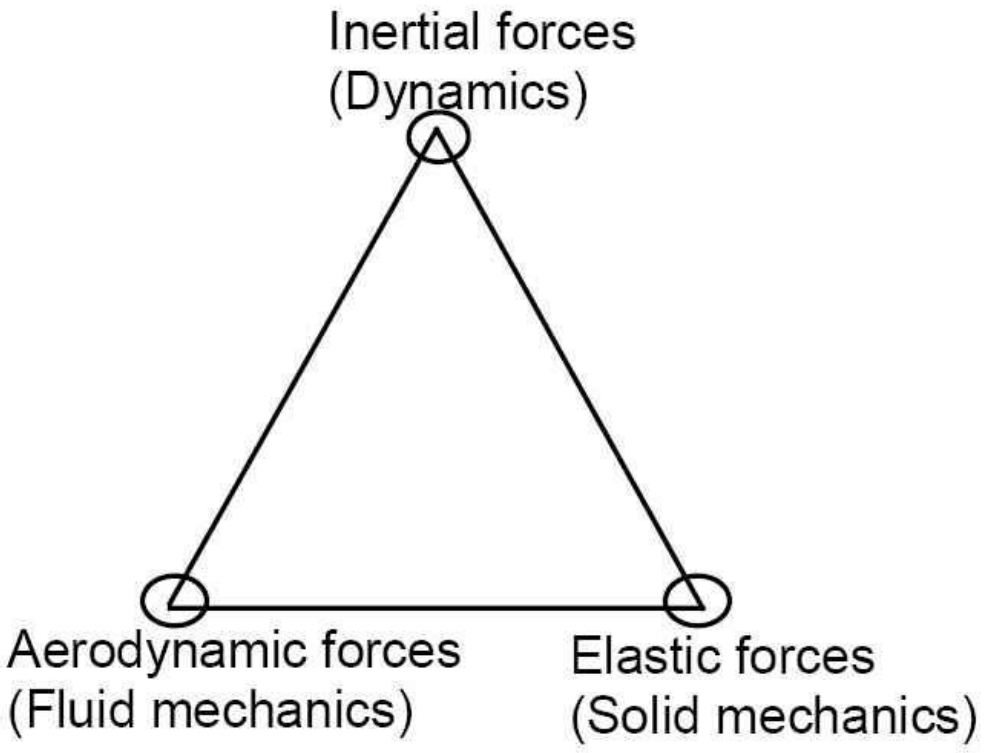

Figure 8 Collar's triangle of forces

In turbomachines, for example turbines, flutter can occur in the rear part of the machine, especially in the last blade stages, due to length of the blade, its slim shape and big aerodynamic forces applied on the blade.

For the important role that the Last Stage Blade plays in transforming energy and efficient of the machine. It is important to study the flutter phenomenon, and improve the methods of avoiding it, design and develop longer blades and more effective blade profiles.

Since the blades stages in turbomachines are established from a row of blades. The influence of Flutter on row of blades will not affect a single blade but the whole row, and each blade has a direct effect on the flow field of neighboring blades in the row. And that is referred to Aerodynamic coupling. Figure 9 shows this effect when flutter happens in blade 0.

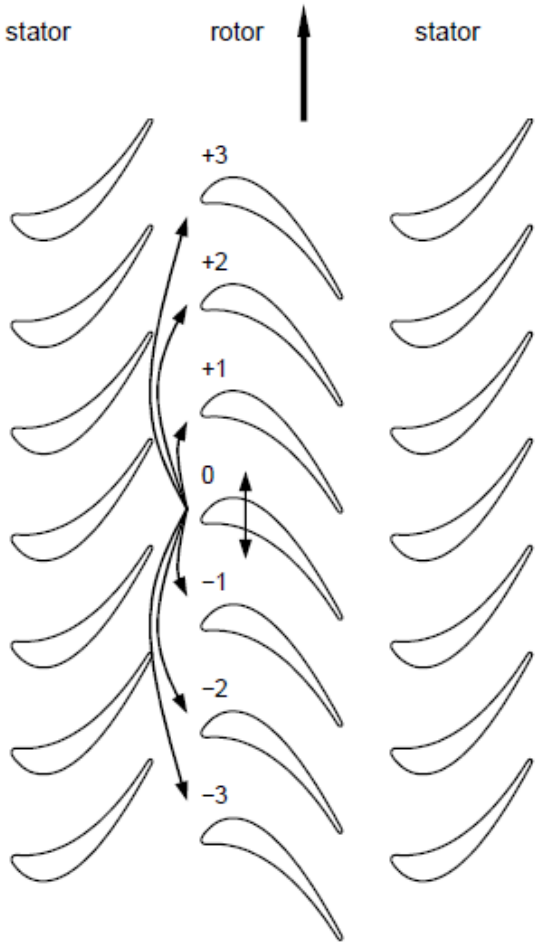

Figure 9 The influence of flutter in a blade on neighboring blades in the row

To understand the coupling phenomena, several studies were made. In a study made by Bellenot and Lalive d'Epinay (1950), it was noticed that the aeroelastic unstable effect could occur in a blade row even though the flutter is not happening in a similar isolated blade from the row. Other studies addressed that in an oscillating blade row, the aerodynamic response is affected by coupling effects.

During flutter in a blade rows, the relative motion between two blades affects the coupling effect, also the blades are oscillating simultaneously with the same amplitude, frequency and mode, but with a specific delay period. This is named as traveling wave mode.

The delay period is called phase lag and it depends on the Interblade Phase Angle (IBPA), and it is given by the equation:

$$\sigma = \frac{2\pi l}{N} \tag{2.1}$$

Where l is the order of traveling wave $l = \{1,2,3, \dots N\}$, also represents the nodal diameter, Figure 10 shows an example of nodal diameter with two different orders

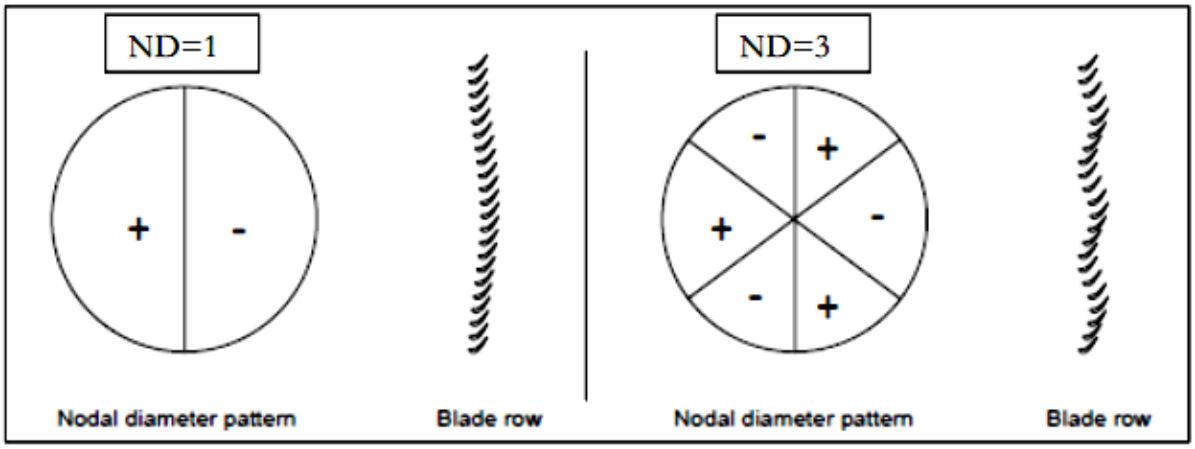

Figure 10 Nodal diameters of a disk, traveling wave mode shape and corresponding instantaneous blade row geometry

In order to study the flutter, some parameters and equations were studied. First, the mass ratio, which is the ratio between the blade mass and the surrounding air or medium in a radius equal to half of the chord. It is shown in Figure 10 and given by the equation:

$$\mu = \frac{4m}{\pi \rho_0 C^2} \tag{2.2}$$

From the equation, m is the mass per unit blade span, ρ_0 the medium density and C the blade chord.

We can find that reducing of the mass ratio leads to increasing of flutter, this ratio has a big values in turbomachines. Study made in 1946 by Meldahl found that the flutter in blade rows happens over certain velocities although the parameters that dominate its stability.

Another ratio used in flutter studies, this ratio presents the time a fluid particle takes to pass the chord of the blade to the period of oscillation:

$$k = \frac{t}{T} = \frac{2\pi f C}{u} \tag{2.3}$$

This is called reduced frequency, where u is the velocity of flow and f is the oscillation frequency.

Another though equivalent interpretation of the reduced frequency is that it relates to the blade chord to the wavelength drawn out by a sinusoidal oscillation as given by

$$k = \frac{C}{\lambda}, \text{ where } \lambda = \frac{u}{\omega} = \frac{u}{2\pi f} \tag{2.4}$$

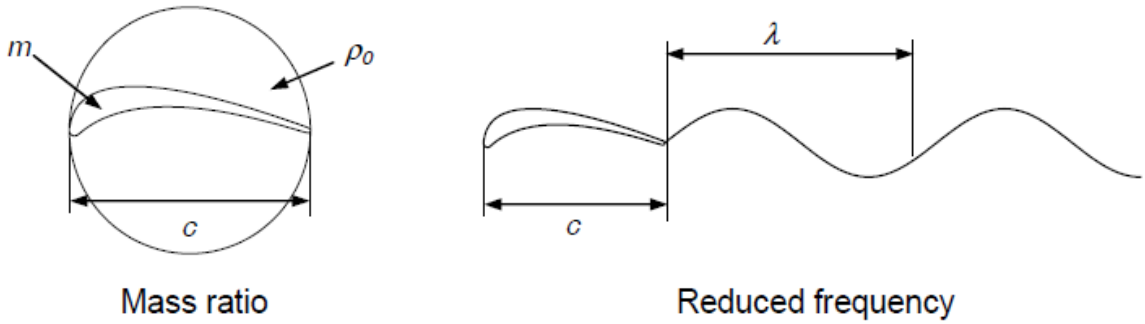

Figure 11 Graphical interpretation of mass ratio and reduced frequency

In Figure 11, notice that the less the value of reduced frequency is, the shorter the time of flight is. The range of reduced frequency in turbomachines is varied from 0.1 to 1.0

Campbell diagram shown in Figure 12 is used to determine and show the relation between the frequency and the rotor speed with various excitation orders versus different torsional frequencies, it describes the characteristics of the structural oscillation. This diagram is used to know the conditions, where the flutter occurrence is, and in design stage.

Notice the flutter occurrence is not related to the order of the engine and can happen at any rotational speed that means additional parameter is still unknown.

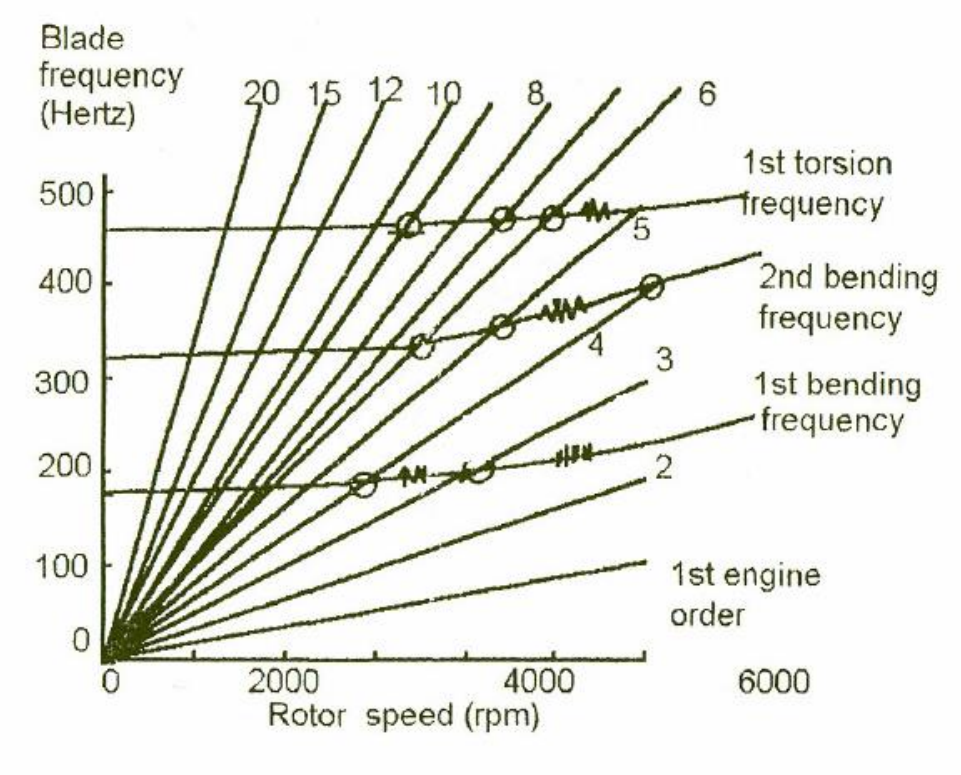

Figure 12 Campbell diagram

Back to the structural effect on flutter, the assembly of blades in a row affect the flutter; it depends mainly on the end of the blades, shrouded and unshrouded, Shrouded blades means that the blades are connected to each other above the root by part span or full span. And unshrouded blades means that the blades have free standing and are not connected to each other. Figure 13 shows the shrouded and unshrouded blade rows.

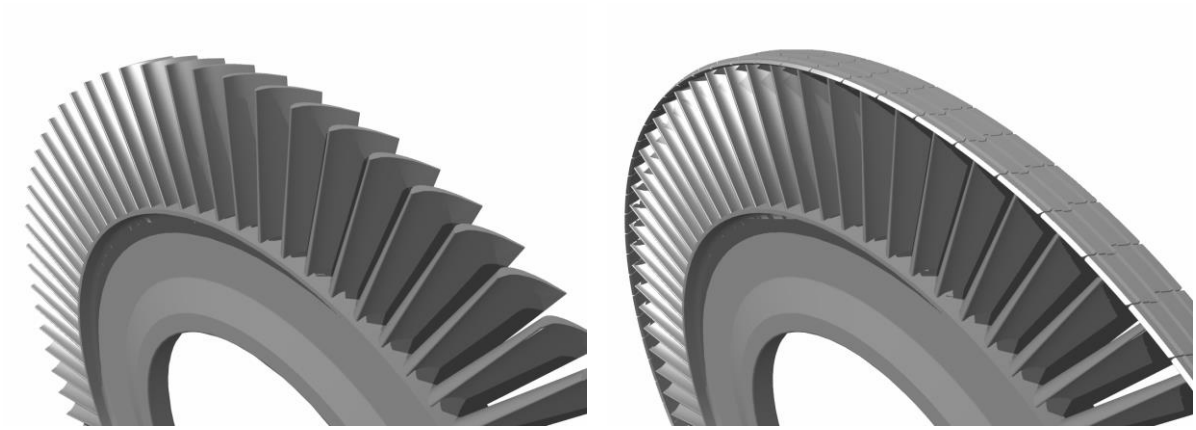

Unshrouded Shrouded

Figure 13 Unshrouded and shrouded bladed disk assemblies.

In unshrouded blade rows, the oscillation of the blades is divided into blade-dominated or diskdominated modes. The blades in diskdominated mode have a passive or secondary role, it is seen as an attached element to the rotor disk. The blade dominated mode contains the bending, torsion and local blade modes as for example corner modes or stripe modes. The blades can vibrate in low frequencies in three different ways, two of them are bending and one torsion. Figure 14 shows this vibration modes, flap and edgewise bending are bending vibrations.

All modes feature a certain eigenfrequency at rest, which changes with the rotational speed of the turbomachine due to centrifugal forces. Other modes include stripe mode (in-plane oscillation) as well as local deformation modes such as corner modes.

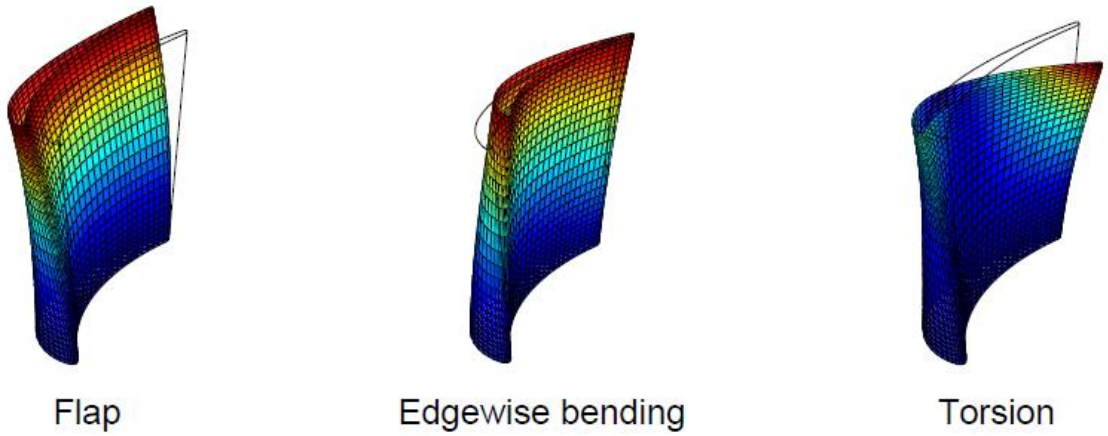

Figure 14 Blade first-order eigenmodes deformation

Connecting the blade ends with shrouds to get more structural stiffness is used to avoid flutter, apply more kinematical constraints that leads to increase the restriction of the coupling of the blades to limited Interblade Phase Angles. Figure 15 shows the oscillation of shrouded blade assemblies given by Ewins (1988).

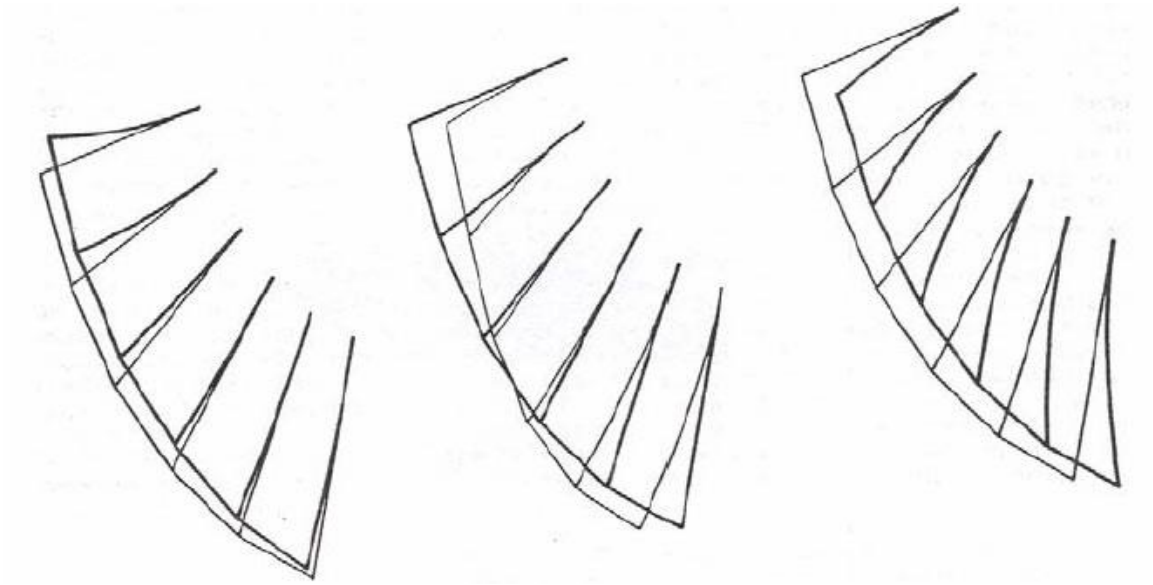

Figure 15 Possible vibration modes for blade packages; from Ewins (1988)

Using of Structural coupling in blade rows might cause combined oscillation of two modes, this case can occur under a certain phase angle and it negatively affects the aeroelastic stability. A study made by Försching (1991) explained the effect of phase angle between bending and torsion mode. For an IBPA = 0^o, the overall work for a cycle is equal to zero, and for IBPA = 90^o, the overall work has positive value. Figure 16 shows this effect and overall work given by Försching.

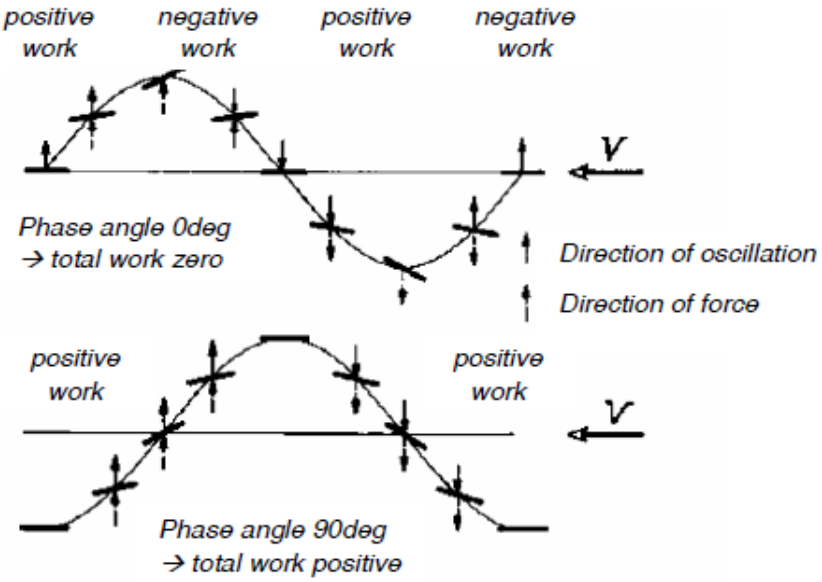

Figure 16 Effect of phase angle between bending and torsion mode on the aerodynamic work performed; adapted from Försching (1991)

The influence of flow incidence affects the aeroelastic stability in an assertive way added to reduced frequency and mode shape. The mean loading of the blades is affected by the flow, as well as blade rows. In general, the higher angles of attack reduce the stability, and the flow might separate around the leading edge above certain angle of attack and that separation leads to aeroelastic stability controlled by the separated flow behavior.

As a result of oscillation, a pressure difference is created up- and downstream of the blade row, which leads to acoustic resonance. And thus we can distinguish three regions of acoustic resonance flutter:

1) Subcritical flutter where acoustic waves cannot propagate in the duct

2) Acoustic resonance flutter where a pair of waves are just at the verge to propagate

3) Supercritical flutter where at least one pair of waves can propagate.

The existence of acoustic resonances can only happen over an exact values of interblade phase angles where the traveling wave mode pattern and resonance pattern matches. In addition, the acoustic resonance adds one degree of freedom to the aeroelastic system, and this degree could be effective for special coupling of blades during flutter. The acoustic resonance flutter has a relevance to empty ducts next to blade row, since the neighboring blade rows try to break this resonant attitude.

In the turbomachines, where there is more than one single blade row, it is clear that the neighboring blade rows have an influence on the flutter. First, it increases the disturbances of the flow, added to the unsteadiness produced by the oscillation of the blade row. By this diffusing the line between flutter and forced response. Also the neighboring blade rows has an influence on the aerodynamic coupling since it can reflect pressure waves. Figure 17 made by Hall et al. (2003) shows the effect of multistage coupling, it shows the results of a single blade row compared to multistage blade rows results using 2D models. Reflection and transmission properties from neighboring blade rows were thereby computed from isolated blade row analyses. In the range from 90^{o} to 180^{o} of Interblade Phase Angle (IBPA), a significant differences are visible.

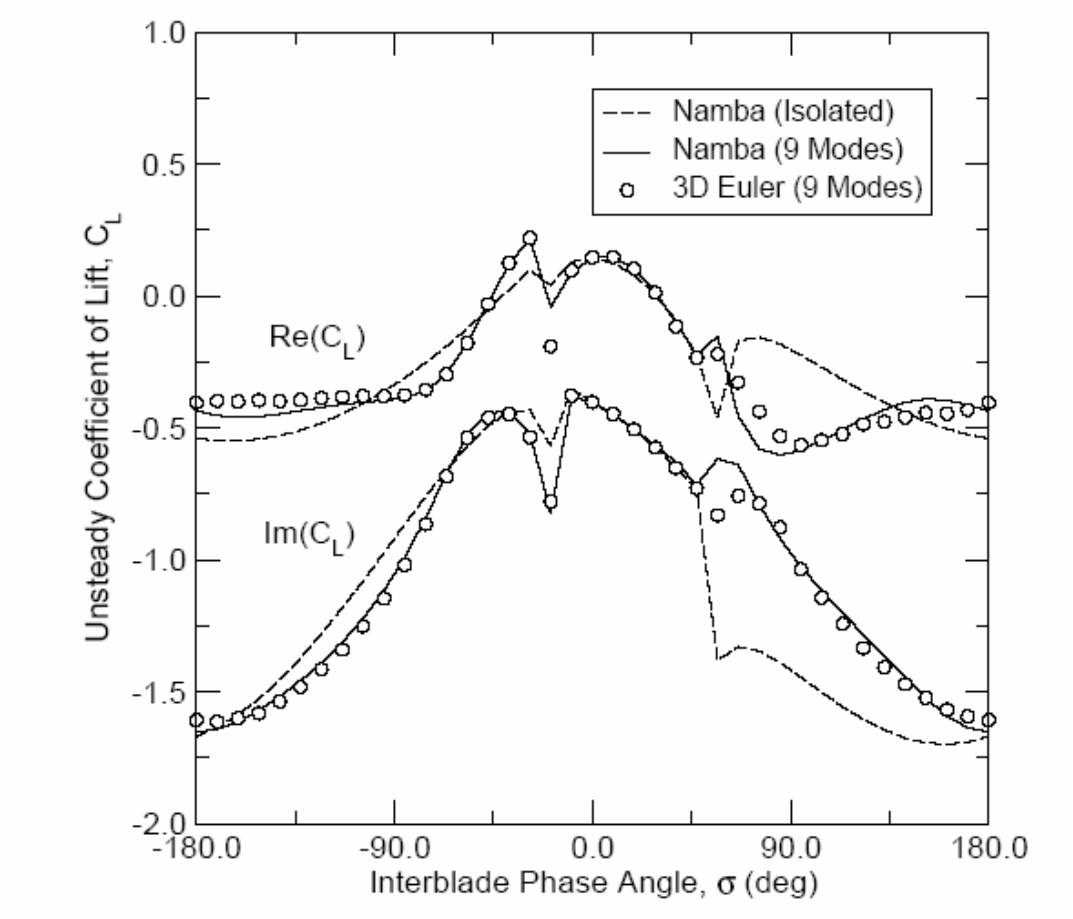

Figure 17 Effect of multistage coupling on flutter stability (2D simulations); from Hall et al. (2003)

2. Flutter testing methods

Testing of flutter is made by two main method, component basis or engine test, component test method is less complicated than full engine test method and gives a close look and analysis of the flutter, but it is less accurate due to the idealization of environment, which leads to missing of some effects that create flutter, for example, in the cascade test, the effect of the neighboring blade rows does not exist.

Since the occurrence of flutter is not stable and the system has a vibrating system that contains fluid flow and structures. Tests of flutter aim either to determine the transfer function of the system using a range of vibration parameters. This test is using forced vibration and excite the system in a controlled way, the response is monitored to determine the transfer function, the second test method aims to detect eventual instability of the system, and in this test is used free flutter type with outer parameters (velocity of flow, angle of attack) changed until observation of flutter.

1) Free flutter test:

Free flutter test aims at observing the occurrence of flutter under special flow conditions, the object of study is exposed to a fluid flow defined parameters and measuring the aerodynamic response and the possibility of flutter vibration. This method can be used in real engines or test frames, for example annular rotating rigs, but this way is not often used due to the complexity and the high costs of performing the experiments. Other ways is to perform this method in simpler cascades. Simpler cascade tests are more cost effective and give the required results.

In some tests, where the aim is to determine the aerodynamic damping characteristics, the aerodynamic forcing is increased in comparison to structural damping, this can be done either by increasing the aspect ratio of the blade or by elastically suspending of blades. Also a variable spring constant of the suspension and mass of the blade is made to observe and measure the aerodynamic damping. In order to observe the oscillation of the blades, strain gauges are used and as an alternative it is used optical techniques.

The test facilities for this method could be full-scale or modeled scale test. One of the facilities made for full-scale flutter studies is in Compressor Research Facility (CRF) at Wright Patterson Air Force Base. Manwaring et al. (1996) studied the effect of inlet distortion on the forced response in a two-stage low aspect ratio fan. Sanders et al. (2002) found the flutter properties of a transonic low aspect ratio fan. As a result, it was found that the main inducer of mistuning are the structural dynamics.

Another study made by Bellenot and Lalive d'Epinay (1950) used a linear cascade with five low-pressure compressor profiles that differ in the aspect ratio from its counterparts in the real machine in order to assist the influence of aerodynamic forcing. The results proved that above a certain velocity flutter was observed, which confirm the validity of reduced frequency on the flutter phenomenon.

For the turbine cascade, Urban et al. (2000) used a seven bladed linear cascade of last stage profiles of steam turbines. To allow torsional oscillation, the blades were elastically suspended as shown in Figure 18 with the center of torsion being located upstream of the leading edge. Blade motion was monitored by means of strain gauges. Moreover, the blades were equipped with miniature pressure transducers such as to provide information on the unsteady loading during flutter.

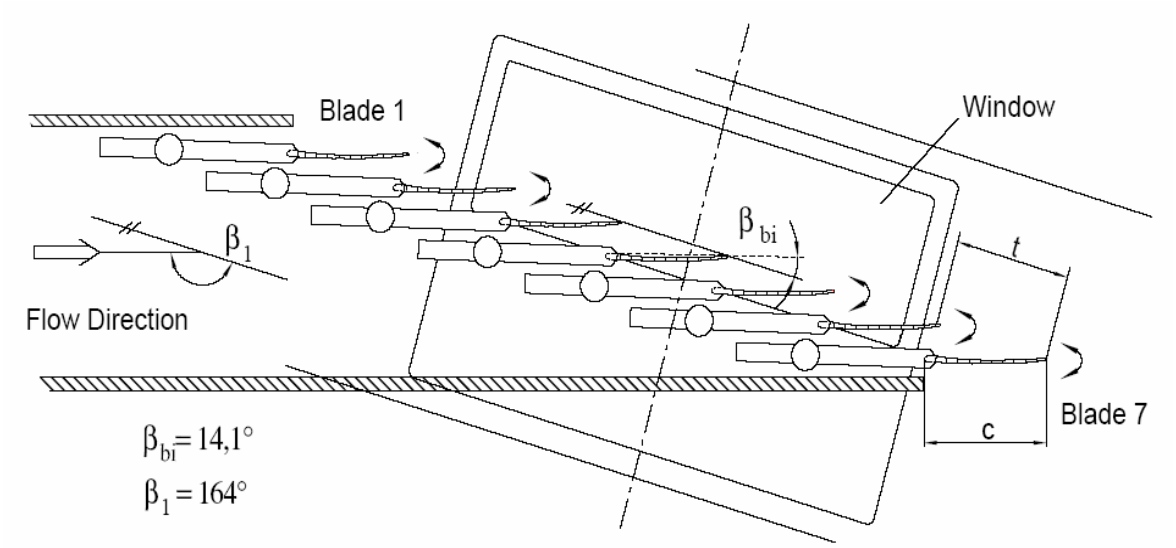

Figure 18 Free flutter test setup for Turbine cascade last blade stage; Urban et al. (2000)

As mentioned above, the free flutter test is less complicated than the controlled flutter test. On the other hand, it has some disadvantages. First of all, in case of no flutter, we could not obtain about the aerodynamic damping, that means no data about the sensitivity of the system.

Secondly, flutter data are available only in case of the least stable condition, that means the data is only obtained at the least stable Interblade Phase Angle (IBPA).

Thirdly, since this method use some cascades with restrictions to some oscillation modes, the flutter data then is only obtained for that specific modal dimension of the system.

Some studies like; Hennings and Send (1998) were able to avoid these disadvantages by using a linear cascade of elastically suspended compressor airfoils undergoing torsional motion. These airfoils could be used in both free oscillation and excited mode. By oscillating one blade using oscillator; which reduces the blade displacement to eigenvectors. This also explains the aeroelastic stability by frequency response functions.

2) Controlled flutter testing:

Controlled flutter test is mostly done by exciting the system through vibrating the blades, in this case, the object of test is oscillating in a controlled manner while it is exposed to fluid flow and the result of aerodynamic response is collected.

Another way is exciting the system by aerodynamic disturbance forces. Here, the object is exposed to fluid flow and the aerodynamic disturbance forces is letting the structure to oscillate freely. Data from the test is concluded from the oscillation properties of the structure.

In control flutter testing use two methods for testing:

- **Traveling wave mode testing**: in this method, all blades in the cascade are oscillated at a defined mode shape and various interblade phase angles. But at only one blade, the response is observed.

- **Influence coefficient testing**: this method uses the oscillation at only one blade and measures the response on all the blades in cascade. The data is observed at different interblade phase angles according to the theory presented below such as to yield damping data in the traveling wave mode domain.

Traveling wave mode and Influence coefficient testing as a method have many advantages and disadvantages. Traveling wave mode is believed to be among the most accurate methods when testing in an annular cascade and perform the circumstances in real engines, this setup is expensive and complex because of the complexity of annular cascades and the way of oscillating such blade in a controlled matter. But also, the pressure waves can freely grow in circumferential direction. That's leads to observance of acoustic resonance.

Bölcs and Fransson (1986) have used an annular non-rotating cascade. This cascade can investigate flutter phenomenon in both compressors and turbine cascades by oscillating one blade or all blades. Moreover, both subsonic and transonic flow conditions could be operated and oscillation of blades is achieved by using a spring type suspension of the blades that are submitted to electromagnetic excitation.

Figure 19 shows the annular non rotating cascade studied by Nowinski and Panovsky (2000) and elastic blade suspension studied by Kahl and Hennings (2000).

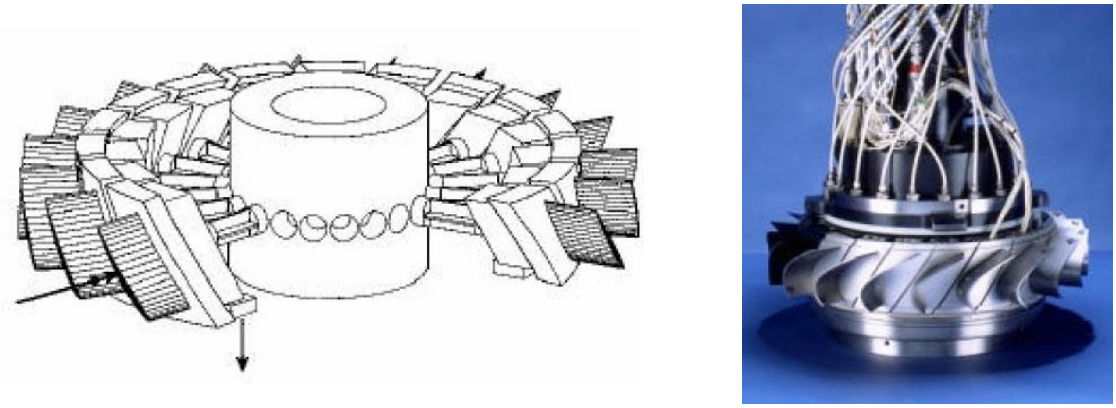

Figure 19 Annular cascade for traveling wave mode and influence coefficient testing

Another type of annular cascade has been used by Frey and Fleeter (1999) for the investigation of combined gust and flutter in low-speed tests. The facility comprises a three-stage experimental compressor with blades that can be made oscillating in traveling wave mode at frequencies proportional to the rotational speed. Oscillation of the blades is achieved by a cam follower assembly as shown in Figure 20.

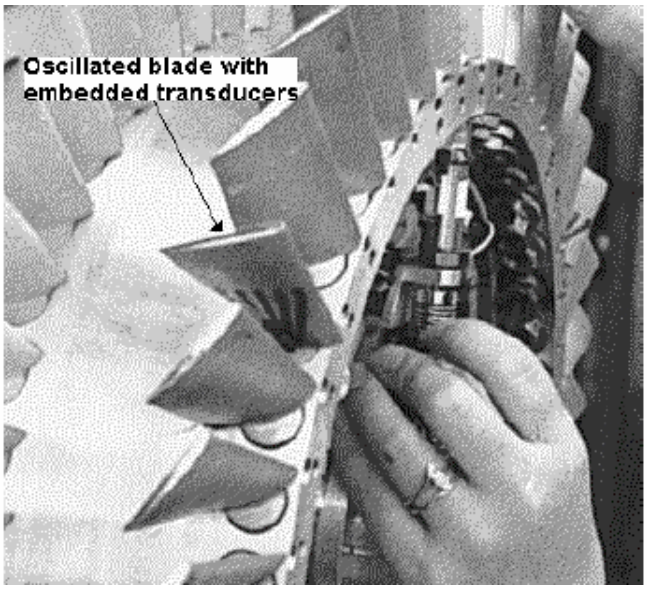

Figure 20 Purdue 3-stage experimental compressor; Frey and Fleeter (1999)

Due to the complexity of annular cascades by using linear cascades, and the complexity of the linear cascades setup the traveling wave mode is used to decrease the test to a simpler level. Thus, the linear cascades are widely used, because the result of the test is easier to compare with 2D results taken from theoretical calculations.

On the other hand, linear cascades have its drawbacks. First, the walls in the unsteady case leads to worsen the pressure wave reflections and avoid the establishment of acoustic resonance flutter. Second, the passage-to-passage periodicity in the steady case, which exist in the annular cascade, must be achieved by means of flow and geometric devices at least in the center passages to achieve acceptance of data.

Several studies investigated these drawbacks. Figure 21 shows a linear cascade of 11 blades, Carta (1983) studied the unsteadiness blade to blade periodicity. It found, that the existence of acoustic resonance was observed at a specific Interblade Phase Angle (IBPA) and that deteriorated unsteady periodicity occurs even with the achievement of a good unsteady periodicity at low speed.

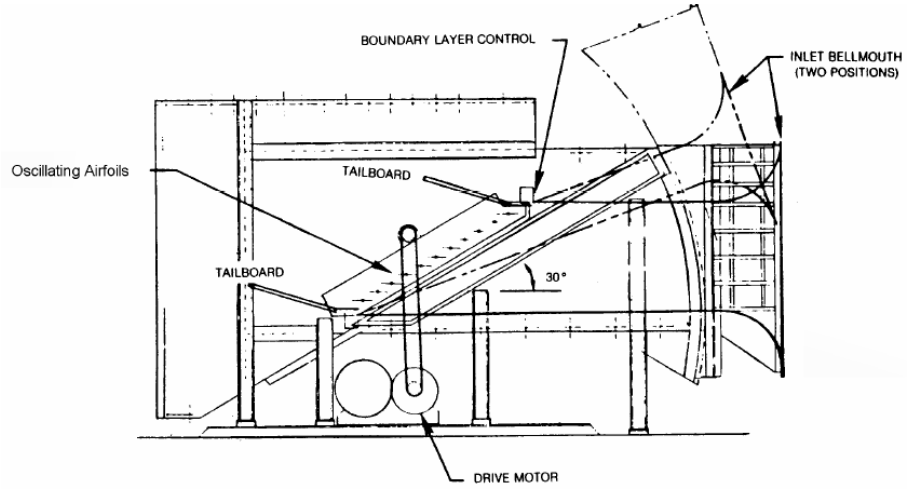

Fig. 21 UTRC Oscillating Cascade Wind Tunnel (OCWT); Carta (1983)

Other studies made by Buffum and Fleeter (1991, 1994) studied the influence on wind tunnel walls on the unsteady performance during flutter, Figure 22 shows the studied cascade at NASA Lewis Transonic Oscillating Cascade where the oscillation is achieved in a mechanical way by cam follower assembly.

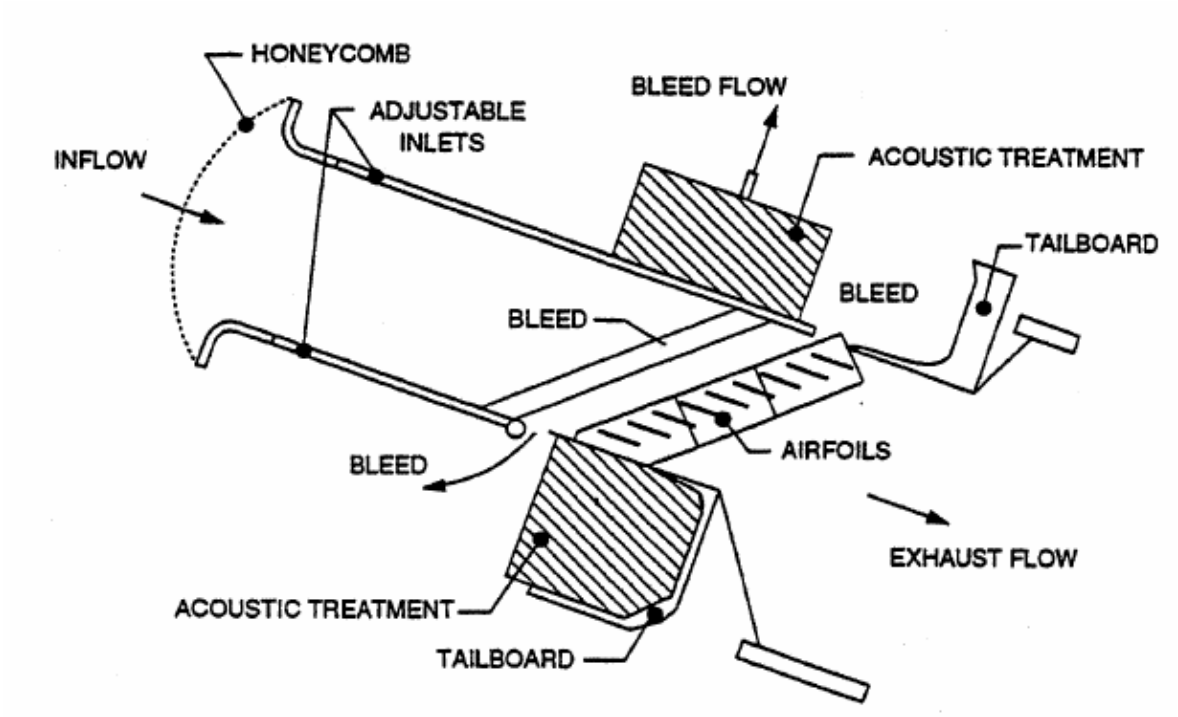

Figure 22 NASA Lewis Transonic Oscillating Cascade; Buffum and Fleeter (1991)

Using the influence coefficient test has many benefits that differ from traveling wave mode, first of all, it is less complicated since only one blade is oscillated. Secondly, the detection of the flutter is more accurate since the blade influence coefficient is determined.

To oscillate the blades, different types of oscillators are used to achieve oscillation parameters, these types aim to produce a controlled oscillation in one or more of the blades with specific frequency and amplitude. The produced modes are mostly 2D modes like rigid body torsional motion or plunging and in all a controlled flutter testing setup the airfoils are oscillated as rigid bodies and not as flexible deforming as their counterparts in real engines.

The main types of oscillating systems can be divided into Mechanical, Electromagnetics and hydraulic. Mechanical system use the rotational movement and transform it into oscillating movement and it is generally the less complicated system among the three systems.

Electromagnetic system is made of electromagnetic shaker and usually contain an elastic suspension, the mode of oscillation is a result of the degree of freedom given by the suspension or in case of several shakers are used from the operation of the shaker setup.

Hydraulic system gives an oscillation mode control similar to Mechanical system, also it gives the highest power density unlike the Mechanical system. The disadvantage is the difficult control in case of high frequencies and loads. Figure 23 shows an example of each system.

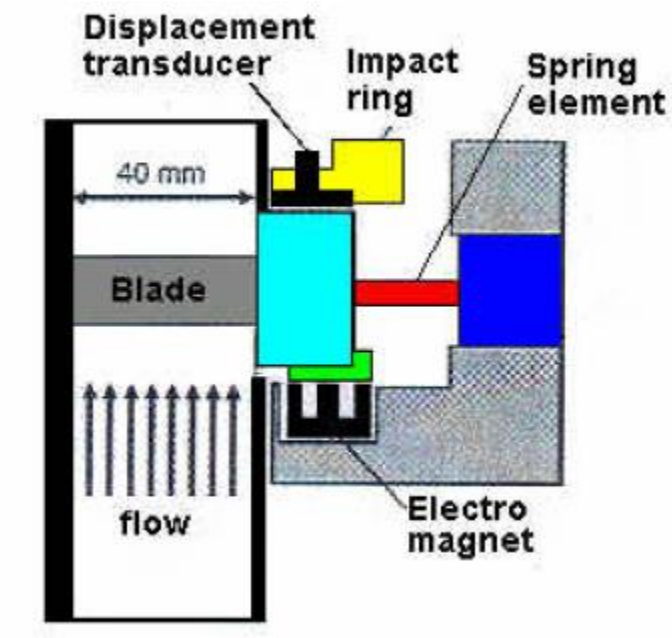

Electromagnetic: EPFL Annular Cascade, Bölcs and Fransson (1986)

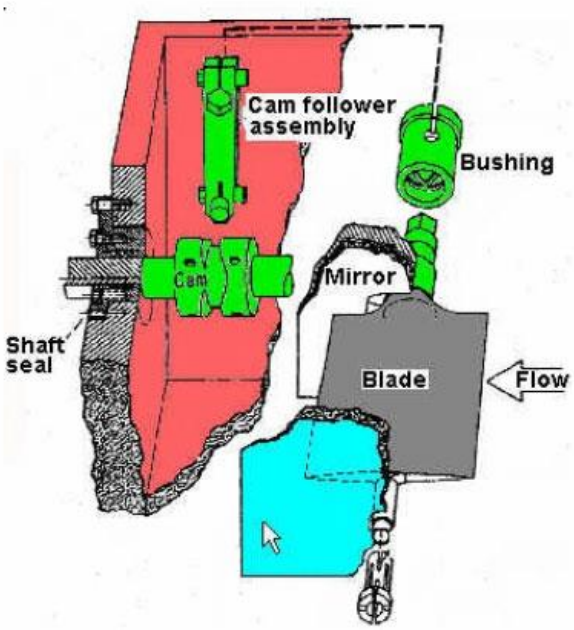

Mechanical: NASA Lewis Oscillating Cascade, Buffum and Fleeter (1991)

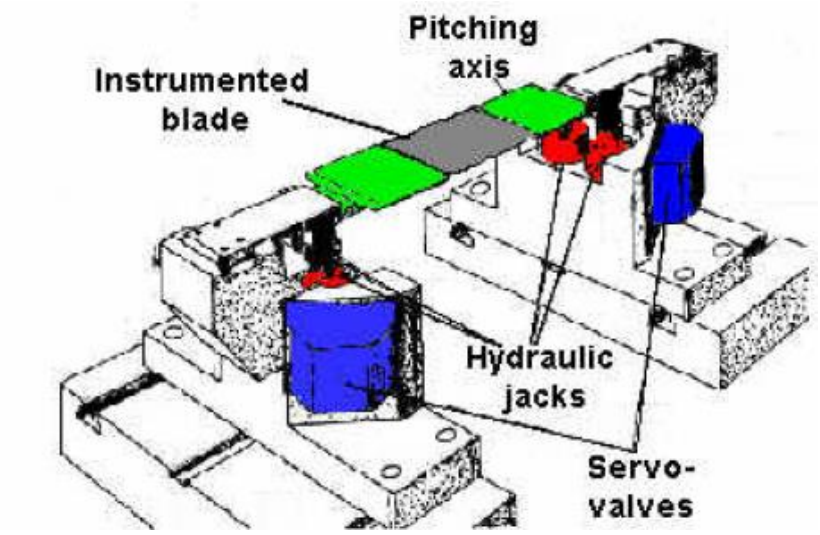

Hydraulic: ONERA Linear Cascade, Széchényi (1985)

Figure 23 Example of type of blade oscillation device

These systems differ mainly in size and power density and depend on the regime of flow in the test rig. It is enough for low speed flows to have oscillating system with moderate frequencies (<50Hz) to achieve relevant reduced frequencies. On the other hand, high speed flows in the high subsonic and transonic regime, require a high speed oscillation system to be able to excite at a higher power density and a higher frequencies of hundreds Hertz.

3 Experimental setup of test rig

An in-draft wind tunnel shown in Figure 24 is used for investigation of aerodynamic and structural stability of a turbine blade cascade. This test rig consists of: Air inlet, inlet filters, calming section, test section, roots blower, air outlet and optional closed circuit. Air inlet is an atmospheric inlet and air enters the system through the filters that avoid any particles from entering the system, after that the air enters the calming section to avoid the air turbulence, then it accelerates in the convergent nozzle before entering the test section.

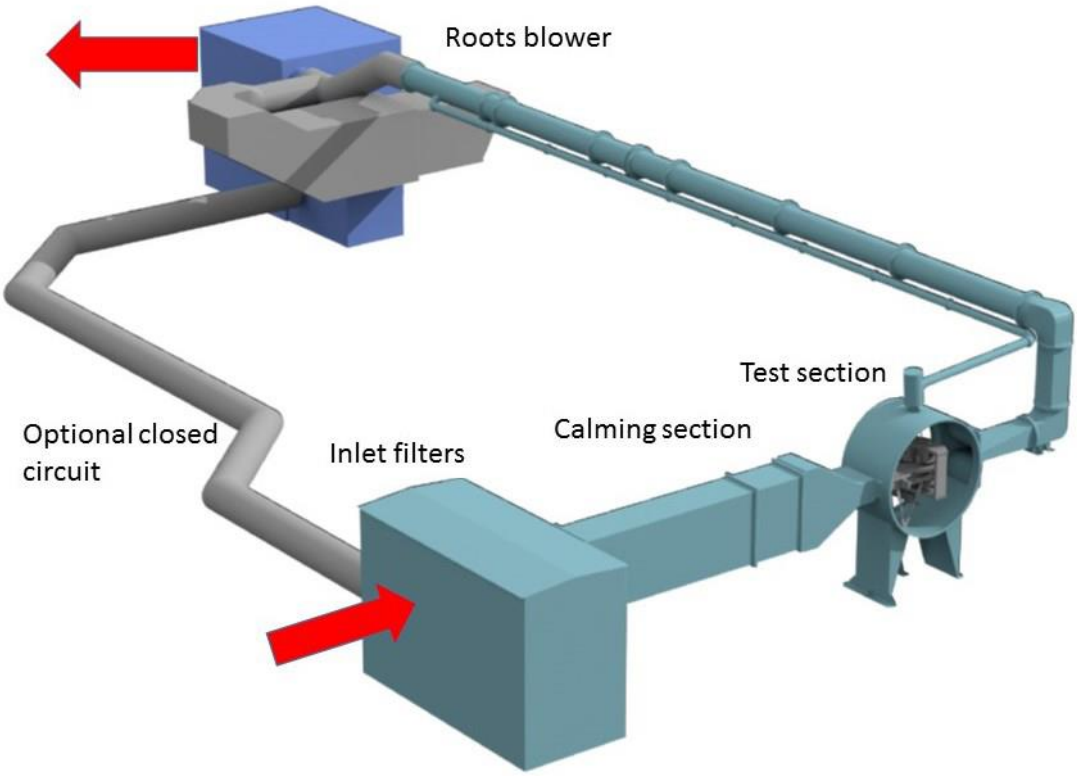

Figure 24 The wind tunnel

The blade cascade and measurements instrumentations are stated in the test section. Blade cascade consist of eight blades in a linear configuration, the central four blades are mounted flexibly and each blade of them has two degrees of freedom presenting torsion and bending motions. In Figure 25 is shown the scheme of the blade cascade, where is stated also the static probe for the measurement of the total pressure and pilot probe for the measurement of the inlet velocity, this probes are situated before the cascade in the upstream of the cascade. And after the cascade (downstream of the cascade) the traversing mechanism with pilot-static probe are situated to measure the velocity and pressure. Inlet flow static temperature is measured using a thermometer sensor situated in the inlet part.

After the test section, the air goes through the outlet duct towards the roots blower pump to the exhaust. As an option, the test rig could operate as a closed circuit and the air goes back to the air inlet section.

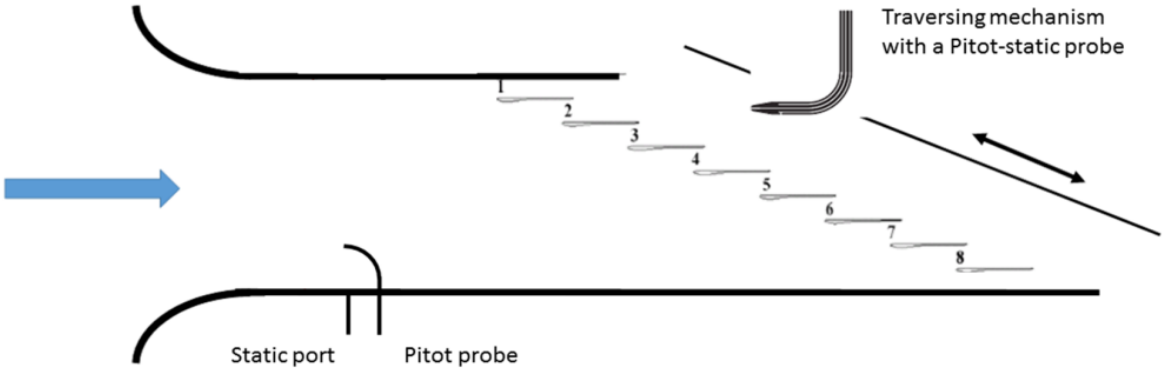

Figure 25 Schematic of the test section, top view with the upstream probes, the linear blade cascade and the traversing plane.

Due to the fact that the aerodynamic forces and moments are small and able to be suppressed by inertial blade loading. The blades are made of carbon fiber, the parameters of the blade cascade are: blade height 80 mm, blade chord 50 mm, maximum blade thickness 2.25 mm, blade pitch 45 mm and cascade stagger angle is 72^{o} .

Figure 26 shown below shows a 3D CAD model for the test section

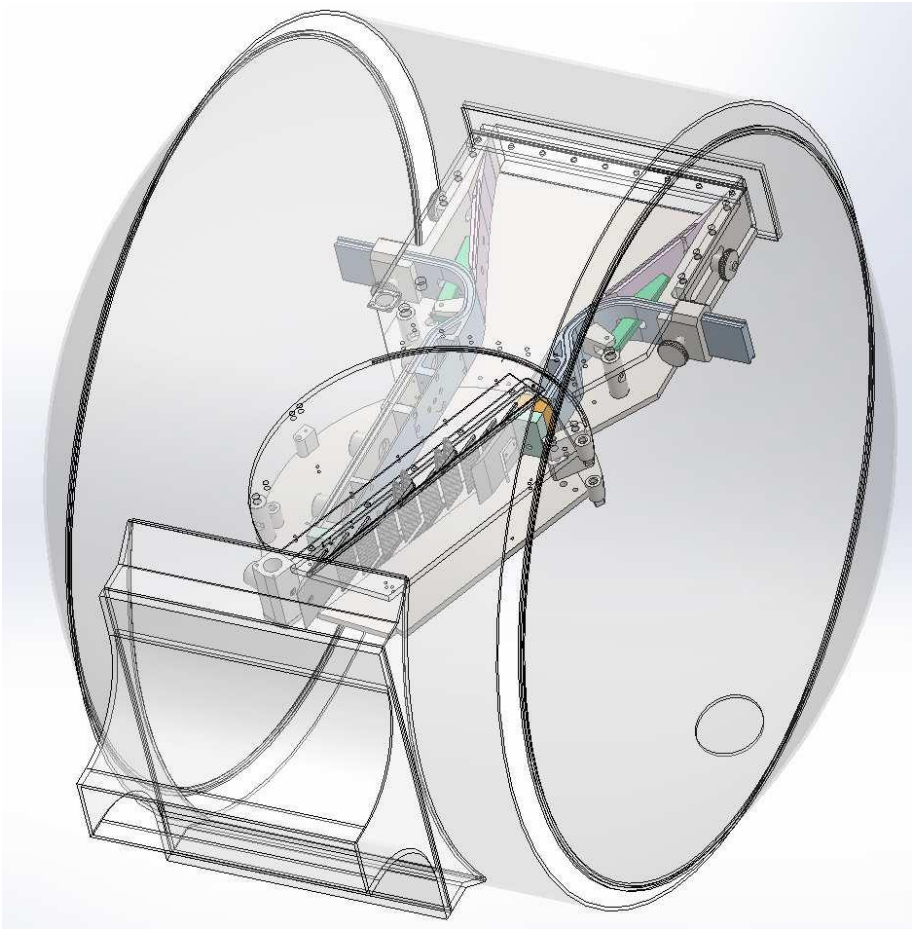

Figure 26 Experimental test section 3D CAD model.

The vibration of the central four blades is achieved by four electromagnetic shakers, these blades are attached at the top and bottom of the supporting frame. Figure 27 shows the way of attaching blades. The position of the supporting frame is adjusted by a lever mechanism in order to avoid the effect of aerostatic loads on the blades and keep constant pitch. Torsion and bending of the blades are provided by an elastic suspension of the electromagnetic shakers. Due to the formation of bending deformation during the measurement of the torsion, a numerical correction of experimental data is performed on rigid blades.

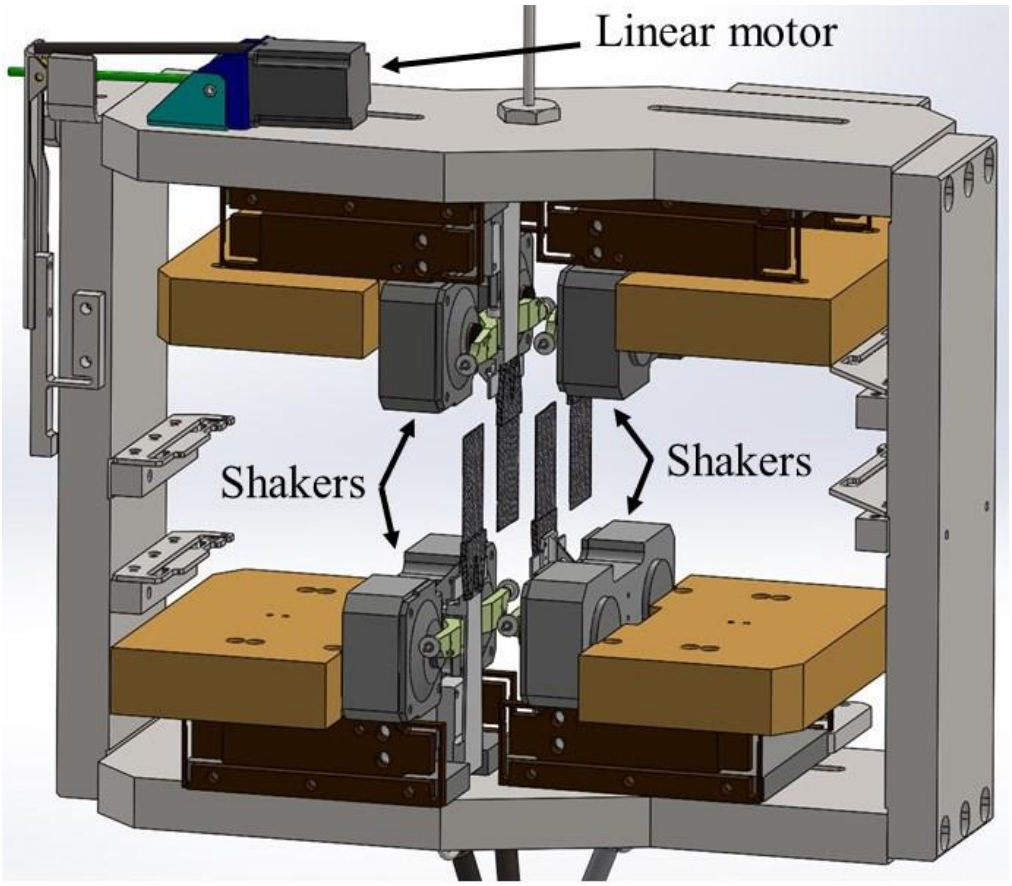

Figure 27 Supporting frame with four electromagnetic shakers.

In Figure 28 shown below, it is seen the blade suspension, it is shown two elastic elements with different widths of the elastic suspension, also notice that the auxiliary elastic element does not prevent the torsion of the main element, both elements create an elastic parallelogram when bending. Along the length of blade, the movement of bending is ideally constant. Two moving coils are partially inserted into larger solenoids. A phase delay between the electric currents running through two moving coils defines the oscillation mode. Each moving coil has a feedback control system to set a precise blade motion.

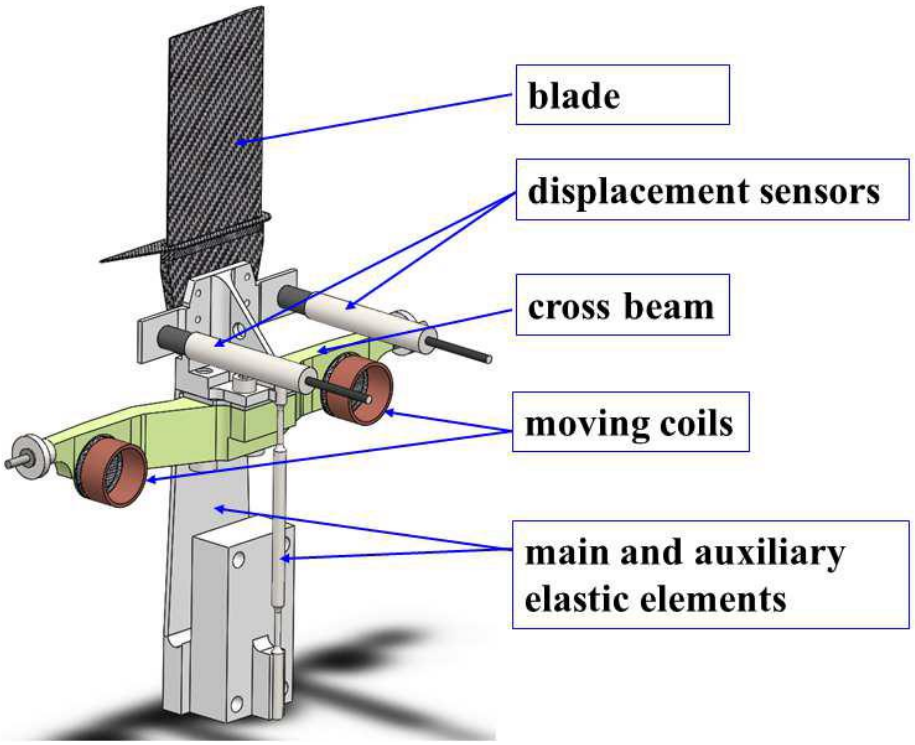

Figure 28 Elastic suspension of the central blades.

Instrumentation and data acquisition

While operating the test rig and by using pitot probe and flush mounted static port, the flow inlet velocity is measured. The inlet temperature is measured by a Thermometer sensor.

In order to measure the pressure profile downstream of the blade cascade, the traversing mechanism was fitted with a Pitot-static probe. All the pressure probes were connected to BHV 5355 differential pressure transducers. Traverser motion is provided by a linear stepper motor. In each position, and in order to avoid transients before sampling of signals, the system was given additional time, signals were sampled with a time duration of 1 second. The mechanism was not able to operate along the full width of the test section due to constructional constraints. Measuring of blade motion was done by using a pair of non-contacting eddy current displacement sensors Schenck IN-085. The bending displacement of blade was observed by a mean of two signals, while the torsion displacement is proportional to the difference of signals. Each sensor has been recalibrated against a metallic measuring surface of the elastic suspension, shown in Figure 28. A simultaneously updating analog output module NI 9264 was programmed in LabVIEW to generate reference signals for eight analog controllers. A NI PXI 1042 chassis with three PXI 4472b modules had been used for a simultaneous sampling of displacement and force signals.

4 Method of measurement

The Aerodynamic loads with arbitrary vibration profiles can be described by forces L, K and moment M, Figure 29 shows the blade cascade used in the test rig with forces L, K and moment M. the effect of force K on X axis is neglected, that means, that force L is measured for the translational oscillation profile (y), and moment M is measure for the angular oscillation profile (α).

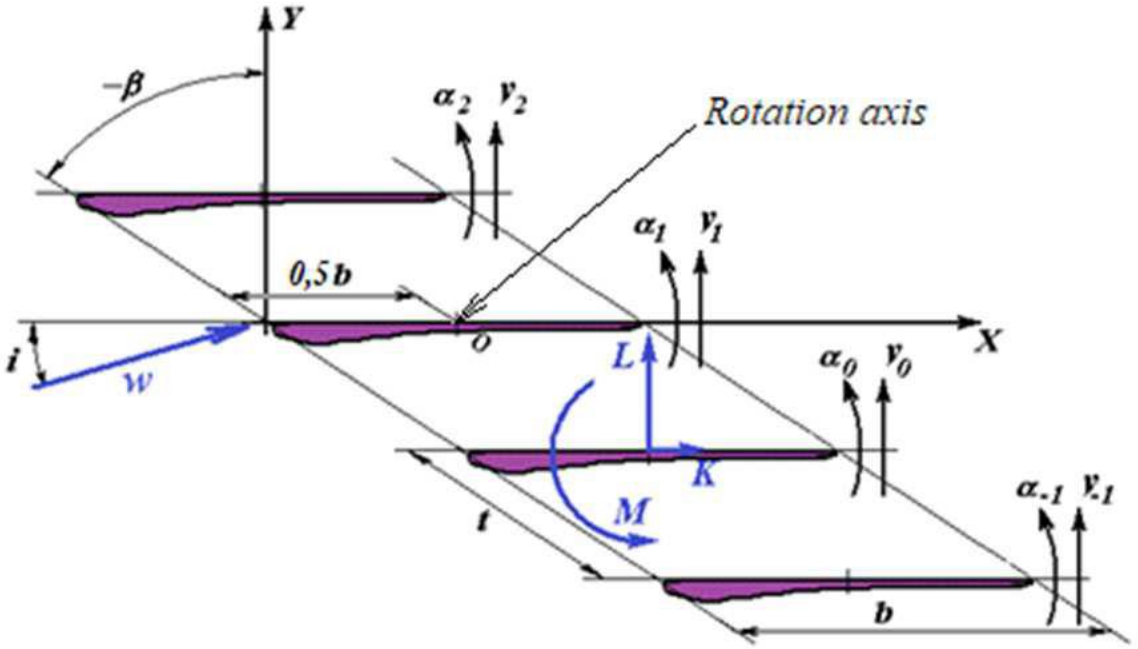

Figure 29 Aerodynamic forces and moment in the blade cascade used in test rig at UWB

In the figure, *b* is the chord, *t* is the pitch, β is the cascade angle, *w* speed of the flow.

The travelling waves of blade harmonic vibration in the cascade can be written in the complex form as in equations 4.1 and 4.2:

$$y_n = |y_n| \cdot e^{-\mathrm{j}n\sigma} \cdot e^{j\omega t}, \tag{4.1}$$

$$\alpha_n = |\alpha_n| \cdot e^{-\mathrm{j}n\sigma} \cdot e^{j\mu} \cdot e^{j\omega t}, \tag{4.2}$$

Where | y | a | α | - amplitude of bending and torsional vibration, *j* is complex unit, *n* is blade number, σ is phase shift between bend and torsion, ω is angular frequency of vibration.

In the case of blade stage, where all blades are identical. The blade amplitude during flutter are constant and also phase shift between the neighboring blades are constant.

Two stationary forces L_{n0} and M_{n0} affect the blades together with the non-stationary (harmonic) force L_n and moment M_n , L_n and M_n are given by equations 4.3 and 4.4:

$$L_n = |L_n| \cdot e^{j\varphi_{L_n}} \cdot e^{j\omega t}, \tag{4.3}$$

$$M_n = |M_n| \cdot e^{j\varphi_{M_n}} \cdot e^{j\omega t}, \tag{4.4}$$

Where $|L_n|$ and $|M_n|$are bending and torsional vibration amplitudes, φ_{L_n}, $\varphi_{M_n}$are phase shifts between the force or torque on the blade n and its respective deflection.

For further analysis, consider that the motion (and hence the load) is harmonic and can be given in the forms:

$$y_n = |y_n| \cdot e^{-\mathrm{jn}\sigma} \tag{4.5}$$

$$\alpha_n = |\alpha_n| \cdot e^{-\mathrm{jn}\sigma} \cdot e^{j\mu} \tag{4.6}$$

$$L_n = |L_n| \cdot e^{j\varphi_{Ln}} = |L_n|\cos(\varphi_{L_n}) + j \cdot |L_n|\sin(\varphi_{L_n}) = \mathrm{Re}(L_n) + j \cdot \mathrm{Im}(L_n) \tag{4.7}$$

$$M_n = |M_n| \cdot e^{j\varphi_{Mn}} = |M_n|\cos(\varphi_{M_n}) + j \cdot |M_n|\sin(\varphi_{M_n}) = \mathrm{Re}(M_n) + j \cdot \mathrm{Im}(M_n) \tag{4.8}$$

Stationary and non-stationary aerodynamic forces and moments are expressed by the equations:

$$L_{n0} = \mathrm{qbhC}_{L_{n0}}, M_{n0} = \mathrm{qb^2hC}_{M_{n0}} \tag{4.9}$$

$$L_n = \mathrm{qbhC}_{L_n},\ M_n = \mathrm{qb^2hC}_{M_n} \tag{4.10}$$

Where $C_{y_{n0}}$, $C_{m_{n0}}$are coefficients of aerodynamic static forces and moments, C_{y_n} a C_{m_n} are coefficients of aerodynamic unsteady forces and moment, h - profile length, q - dynamic pressure.

The profiles are installed on the shakers according to figure 30.

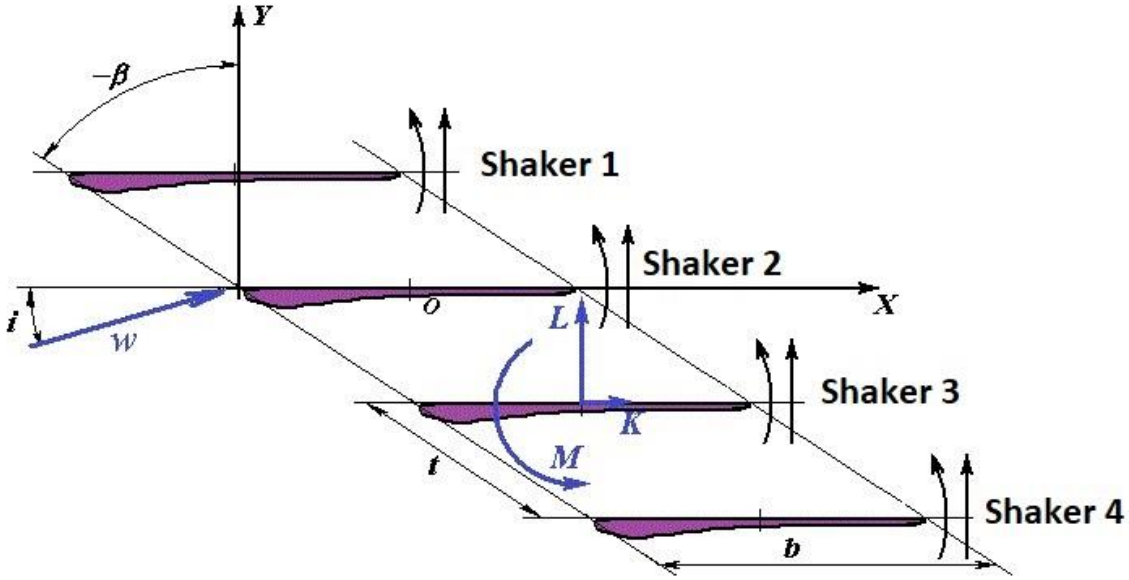

Figure 30 shaker's index

Travelling wave method

The travelling wave mode amplitudes for bending and torsion are given by the equations:

$$y_{\mathrm{nv}} = Y \cdot e^{j(\mathrm{nv}-1)\sigma} \tag{4.11}$$

$$\alpha_{\mathrm{nv}} = A \cdot e^{j(\mathrm{nv}-1)\sigma} \tag{4.12}$$

Where σ is is the phase shift between neighboring blades, μ is the phase shift between bend and torsion, *nv* give the shaker number, IBPA is configured with a step $\Delta=30^{o}$.

Calculation of work of aerodynamic forces and moments in oscillating blades

The work of non-stationary aerodynamic forces and moment in four blades mounted to oscillators is defined as a sum of work from forces of bending oscillation and of work from torsional moments of torsional vibration:

$$W = \pi|y| \cdot |L| \cdot \sin(\varphi_L) + \pi|\alpha| \cdot |M| \cdot \sin(\varphi_M) \tag{4.13}$$

$$W = \pi|y| \cdot \mathrm{Im}(L) + \pi|\alpha| \cdot \mathrm{Im}(M) \tag{4.14}$$

From the equation, the positive work value of aerodynamic loads in a cycle of vibration means that the energy of the oscillation system is increasing because of using of flow energy (destabilizing effect). For further required comparisons between the calculated and experimental results, coefficient C_W, which represents the work of non-stationary aerodynamic loads in a non-dimensional form, it is shown in equation:

$$C_W = \frac{W}{\pi \cdot W_{\mathrm{kf}}} = |\bar{y}| \cdot \mathrm{Im}(C_L) + |\alpha| \cdot \mathrm{Im}(C_M) \tag{4.15}$$

Where $\bar{y} = y/b$, $C_L = C_{L_y} + C_{L_\alpha}$, $C_M = C_{M_y} + C_{M_\alpha}$, $W_{\mathrm{kf}} = \frac{\rho \cdot V^2}{2} \cdot h \cdot b^2$

For clear bending vibration, the work sign is replaced by the component $\mathrm{Im}(C_L)$

$$C_W = \frac{W}{\pi \cdot q \cdot h \cdot b^2} = |\bar{y}| \cdot \mathrm{Im}\left(C_{L_y}\right) \tag{4.16}$$

For clear torsional vibration, the work sign is replaced by the component $\mathrm{Im}(C_M)$

$$C_W = \frac{W}{\pi \cdot q \cdot h \cdot b^2} = |\alpha| \cdot \mathrm{Im}\left(C_{M_\alpha}\right) \tag{4.17}$$

By knowing and having $\mathrm{Im}\left(C_{M_{\mathrm{an}}}\right)$, it is easy to find work

$$W_n = \pi \cdot q \cdot h \cdot b^2 |\alpha_n| \cdot \mathrm{Im}\left(C_{M_{\mathrm{an}}}\right) * 1000 \tag{4.18}$$

Measurement of unsteady aerodynamic forces and moments

The Elastic suspension of a blade with two degrees of freedom is shown in Figure 31 according to Tsimbalyuk (1996), and the aerodynamic loads are secured and developed during flow by the yoke (1)

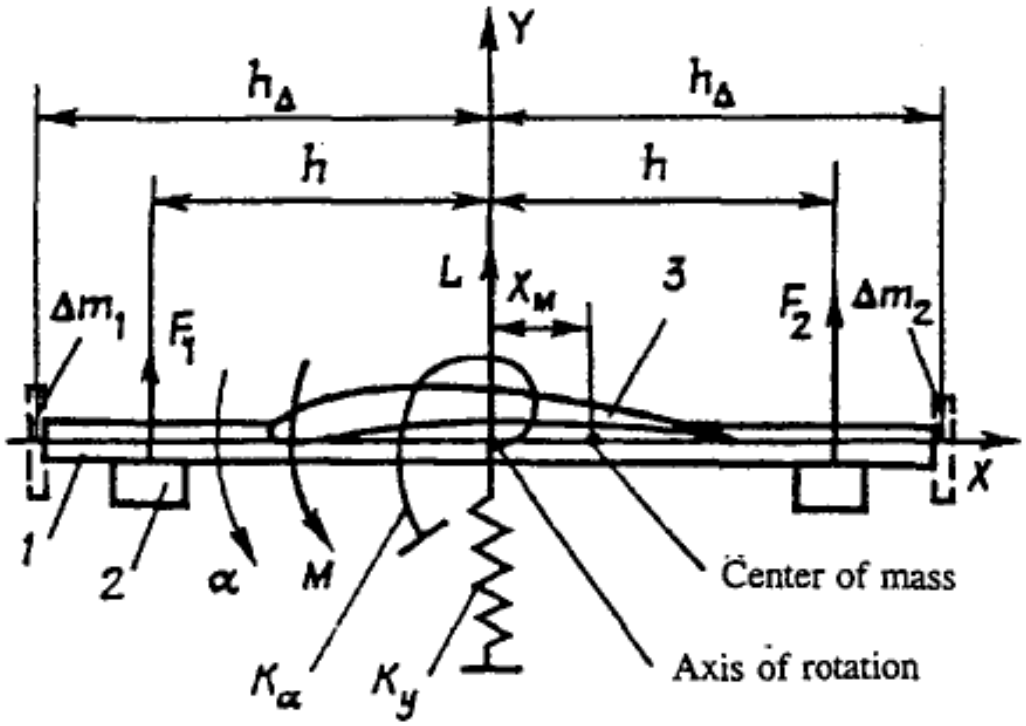

Figure 31 Elastic suspension of a blade, Tsimbalyuk (1996)

The equations can be written in the form:

$$m\ddot{y} + g_y\dot{y} + K_y y + mx_m\ddot{\alpha} = L$$
$$I\ddot{\alpha} + g_\alpha\dot{\alpha} + K_\alpha\alpha + mx_m\ddot{y} = M \quad (4.19)$$

Where m is the mass of the suspension with the blade; I is the moment of inertia relative to the axis of rotation; x_m is the coordinate of the center of mass; K_y and K_α are the stiffness coefficients of the elastic elements; g_y and g_α are the coefficients of structural damping in the corresponding directions.

In order to determine the aerodynamic forces and moments, it is necessary to measure the currents in the moving coils of the vibrators in the presence and absence of a flow while keeping the prescribed vibrations of the vanes unchanged.

Reducing the error of the determination of the aerodynamic loads from the difference in two measurements and improving the sensitivity of the measuring instrument can be done by reducing the aerodynamic force and moment in case of vibration without a flow.

The equation of the aerodynamic forces L and M can be written as a function to aerodynamic influence coefficients as following:

$$L = qc \sum_{n=-1}^{2} \left(\frac{k_{ny} y_n}{c} + k_{n\alpha} \alpha_n\right)$$
$$M = P_d c^2 \sum_{n=-1}^{2} \left(\frac{l_{ny} y_n}{c} + l_{n\alpha} \alpha_n\right) \quad (4.20)$$

Where q is the dynamic pressure, c is the blade chord and k, l are the complex aerodynamic influence coefficients. Subscript y means motion in y direction, subscript α means the torsion in α direction and subscript n is a number of blade.

The aerodynamic forces according to Figure 31 were monitored. The energy method was used to compute aerodynamic forces. It means the aerodynamic force is given by the sum of the surface integrals:

$$L = \int_A p \mathrm{n} \mathrm{d}A + \int_A \tau \mathrm{d}A \quad (4.21)$$

Where *p* is the static pressure on the blade surface, *A* is the blade surface, n is the unit normal vector to the surface *A* and t is the stress vector.

The aerodynamic work, which is used as an indicator of the potential danger of flutter, is defined by the following equation:

$$AW_{cycle} = \int_{t_0}^{t_0+T} \int_A -p \mathrm{Vn}\, \mathrm{d}A\, \mathrm{d}t \quad (4.22)$$

where *T* is the period of one vibration cycle, *t0* is the time at the start of the vibration cycle, *p* is fluid pressure, V is the velocity of the blade due to imposed vibrational displacement (a defined blade motion), *A* is the surface of the blade and n is the unit normal vector to the surface A.

By using equations shown above and by using controlled flutter testing method, the aerodynamics forces and moments can be calculated. It considers a linear model of aerodynamic loading, the oscillators of the blades provide the same vibration of the blade cascade in both flow and no flow cases and the aerodynamic loading can be estimated by the difference between these two measurements.

1- The center of the mass x_m must coincide the axis of rotation:

$$x_m = 0 \quad (4.23)$$

2- The working frequency must be equal to the natural frequencies of translational and angular vibrations of the suspension:

$$\omega_{0y} = \omega_{0x} = \omega \quad (4.24)$$

3- The masses of the vibrating parts of the suspension should be small and the number of joints in the suspension should be minimal in order to make the mechanical damping negligible. This condition will make the vibrating system more stable.

4- Moreover, constancy of the parameters of the vibrations along the blade requires that the first natural frequency of the vane be several times greater than the frequency of the forced vibrations:

$$\omega_p \geq 4\omega \tag{4.25}$$

Figure 32 shows the blade deformation at bending vibration obtained using a Polytec PDV-100 portable digital laser vibrometer. Therefore, blade deflection must be accounted for the analysis of unsteady aerodynamic forces and moments [3].

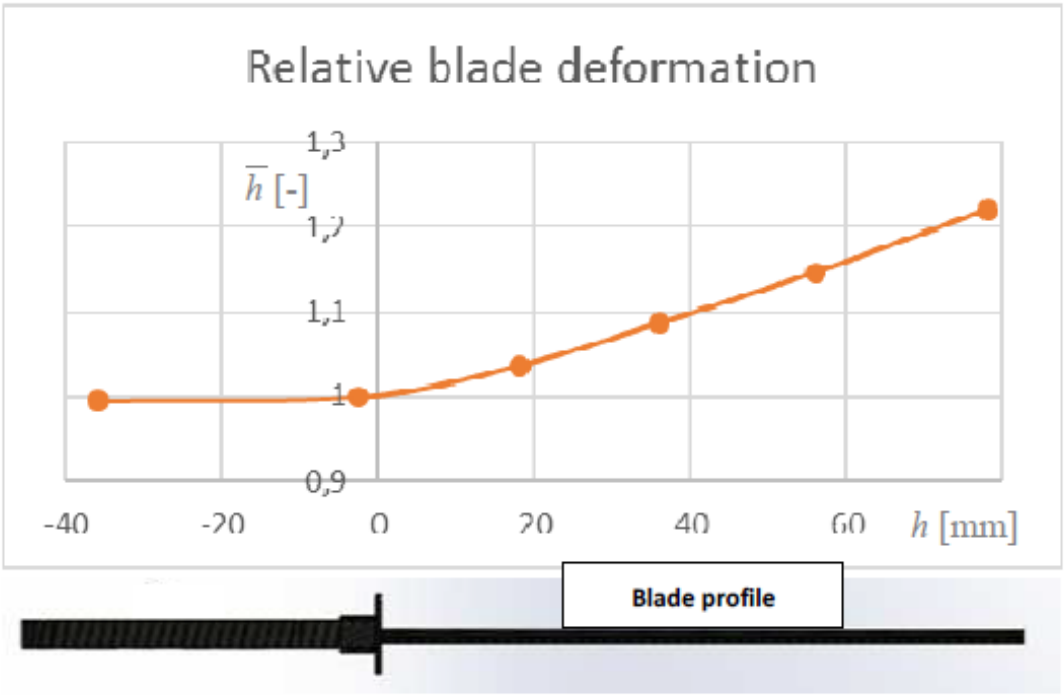

Figure 32 Blade deformation at bending vibration

5 Experimental results

Experiments were carried out using a subsonic wind tunnel based in the Department of Power System Engineering, Faculty of Mechanical Engineering, University of West Bohemia.

Experiments were divided into two parts, stationary and vibrating. Stationary tests are performed by fixing all the blades and measuring the pressure profiles, total and static pressures. While vibrating tests are performed by oscillating the central four blades in the cascade and observe the possibility of flutter occurrence.

Figure 33 shows the blade profile installed in the blade cascade, detailed parameters are stated in Appendix 1

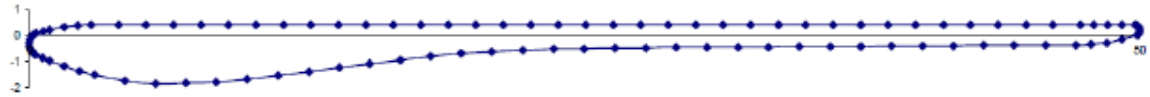

Figure 33 blade profile

Figure 34 shows the main parameters of the blade cascade installed in the test rig, where the maximum thickness of blade is equal to 2.25 mm, chord of the blade is 50 mm, and throat of the cascade is equal to 15.3 mm.

Before starting test, test rig and equipment were checked to assure that they are working correctly, and before starting measurement, the central four blade were adjusted in order to keep the pitch constant.

The whole cascade is shown in Figure 25, and due to construction limits, the tests will show measurement data only from blade 2 to blade 7.

Stationary tests

Four tests were performed to observe the pressure profiles at a different blade heights, different velocities, the first three tests were performed for Mach's number equal to 0.2 , AoA equals to 5°, pressure was measured at the bottom, middle and top of the blades, while the fourth test was performed for Ma = 0.42, AoA= 0°.

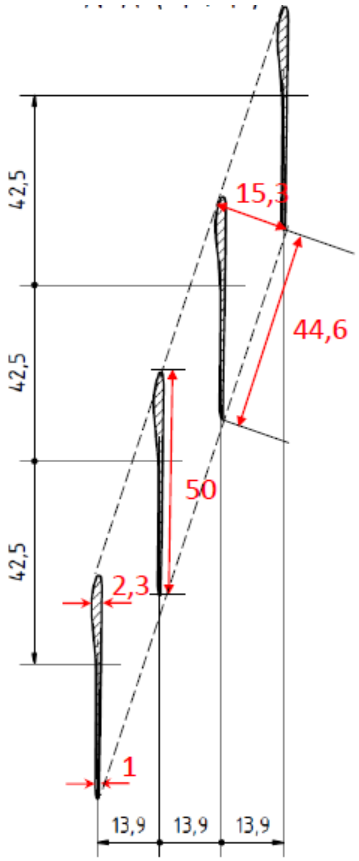

Figure 34 blade cascade parameters

First test:

The first test was performed at **AoA = 5º**, **Ma=0. 2**, and position of the sensors is at the middle of the blade height. The main parameters of the test are shown in table 1:

t_in	**(°C)**	4.52
ps_in	**(Pa)**	97758.42
pc_in	**(Pa)**	100494.1
Ma_in	**(-)**	0.199
m_out	**(kg/s)**	1.01
AoA	**(°)**	5
Position of travers sensor	**(%)**	50

Table 1: main parameters of the first test

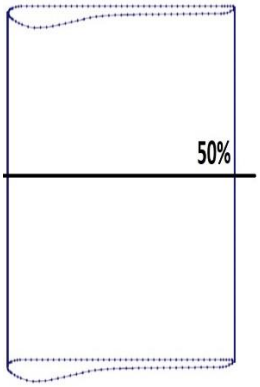

Figure 35: position of the sensors to the blade height

Results of the test are shown in Figure 36

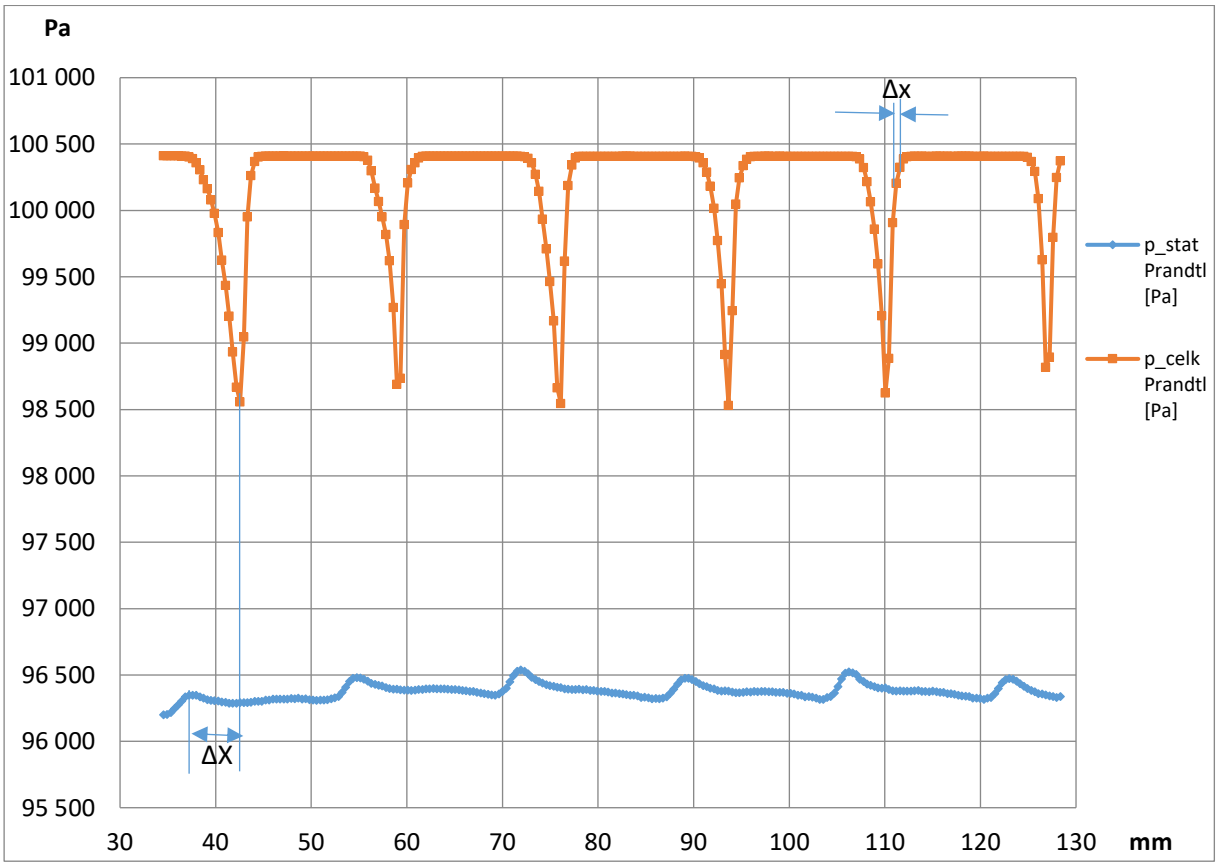

Figure 36 Pressure profile for the cascade at AoA = 5º and Ma = 0.2

From the above figure, notice that the total pressure downstream of the blades in the interblade channels is constant, while it drops in the wakes. Also notice that the static pressure is constant with small peaks that are due to the effect of flow on sensors close to the blade wall. For a better explanation, the distance between the traversing mechanism and the end of the blade is 1.8 mm. when the probes get closer to the trailing edge of blade, the flow goes around the probes and the velocity of the flow between the edge and the probes decreases, and that leads to the creation of the peaks.

In the case of stationary blade cascade, where all the blades are fixed, the pressure loss in the wakes is supposed to be more less constant, while in the results differ, table 2 shows the pressures in the wakes, which show that wakes are in reasonable agreement. The small differences are due to the finite measurement step, which is $\Delta x = 0.3813$ mm. For a better and more accurate results, the measurement step must be smaller. The experiments in this case will take a long time to perform.

blade	P_c [Pa]
2	98556.8
3	98690.3
4	98544.4
5	98531.4
6	98623.7
7	98818.4

Table 2: Values of P_c in the wakes

From the figure it is noticed also a difference between the static pressure peaks and total pressure losses (ΔX), the values of ΔX are shown in table 3:

In order to calculate the pressure loss between the inlet and outlet of the cascade for total pressure and static pressure, two non-dimensional coefficients were used, these coefficients represent the ratio between the total pressure downstream the cascade, respectively the static pressure, to the total inlet pressure of the cascade, this coefficients are given by the equation (5.1):

$$C_{ps} = \frac{P_{sz}}{P_c}, \quad C_{pc} = \frac{P_{cz}}{P_c} \qquad (5.1)$$

blade	ΔX [mm]
2	5.34
3	4.19
4	4.19
5	4.19
6	3.81
7	3.81

Table 3: Values of ΔX

Where P_{sz} is the static pressure downstream the cascade, P_{cz} is the total pressure downstream the cascade and P_c is the total inlet pressure, the results are shown in the following figure:

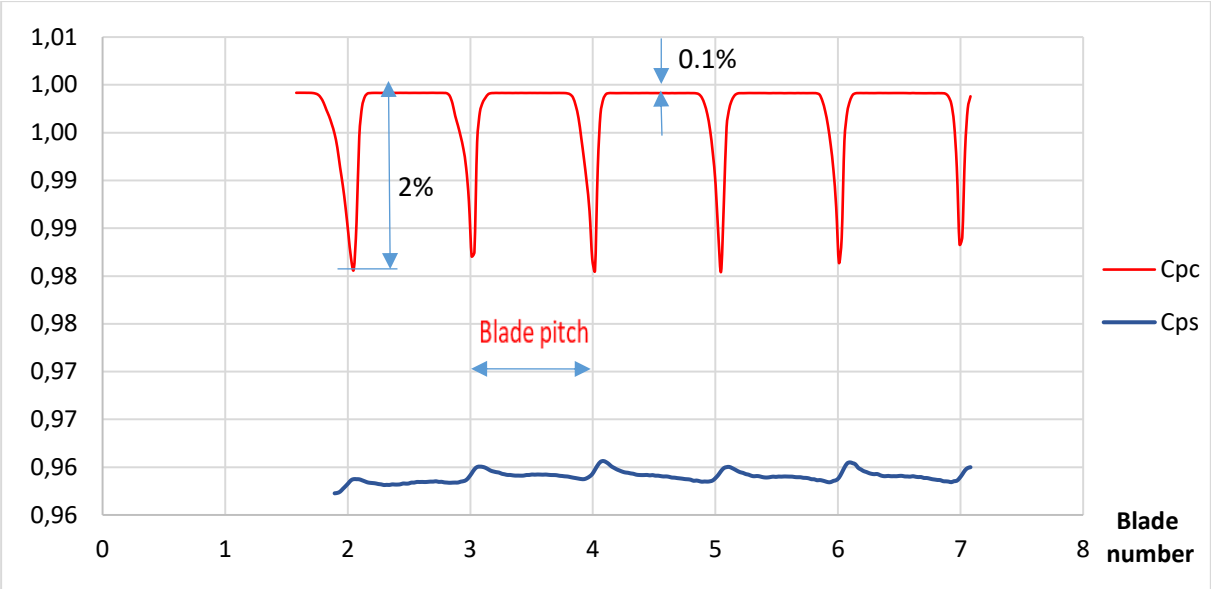

Figure 37 Pressure profile for the cascade at AoA = 5° and Ma = 0.2 using Cpc and Cps

From the figure 37, notice that the coefficient C_{pc} =1 means no pressure loss between the inlet and the outlet, the total pressure loss in the inter-blade channels is about 0.1%, while the pressure loss in the wakes is about 2%.

The dynamic pressure is defined as the difference between the total pressure and the static pressure and it is given by the equation:

$$P_d = P_c - P_s \tag{5.2}$$

The dynamic pressure profile is shown in the following figure 38:

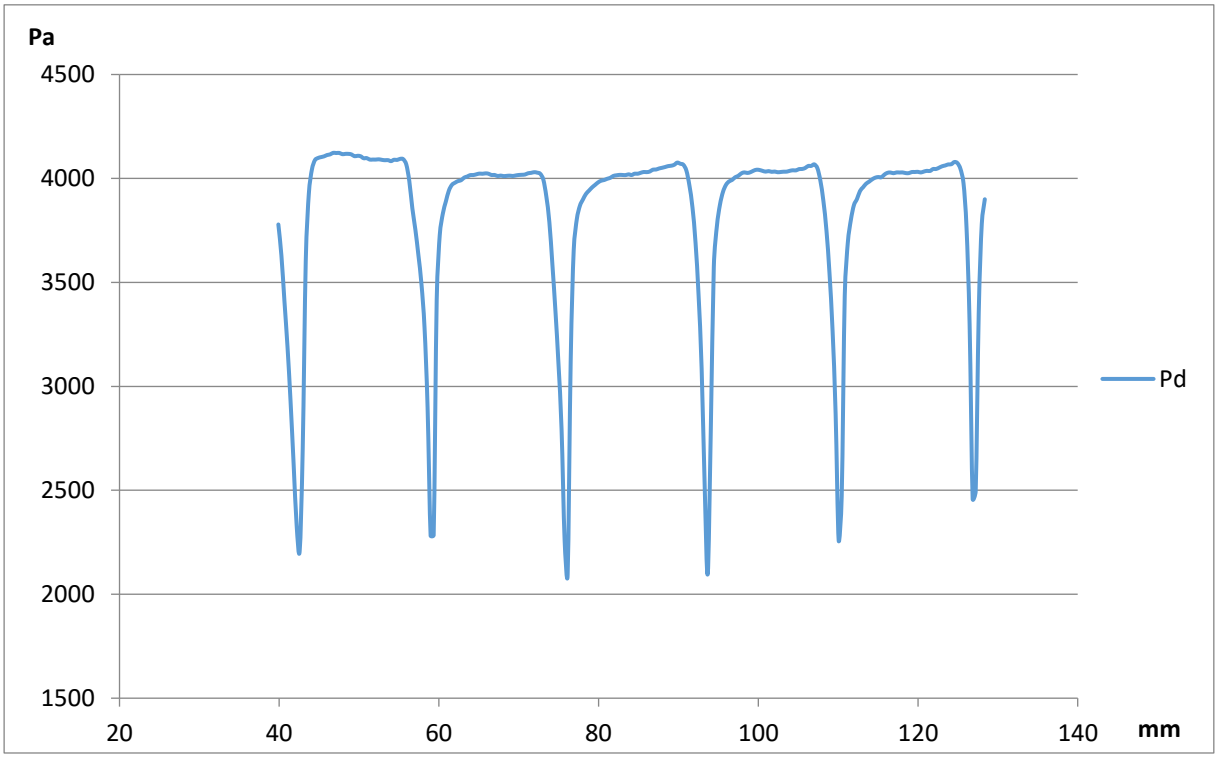

Figure 38 Dynamic pressure profile for the cascade at AoA = 5° and Ma = 0.2

The velocity of the flow "u" is calculated by the following equation:

$$P_d = \frac{1}{2}\rho u^2 \tag{5.3}$$

Where ρ is the density of the medium and it can be calculated by the equation:

$$P = \rho rT \tag{5.4}$$

Where $P = P_s$, $r = 287.15\ \frac{J}{kg.K}$ and T is considered to be equal to T_{in} for Mach's number less than 0.3 , figure 39 shows the velocity profile:

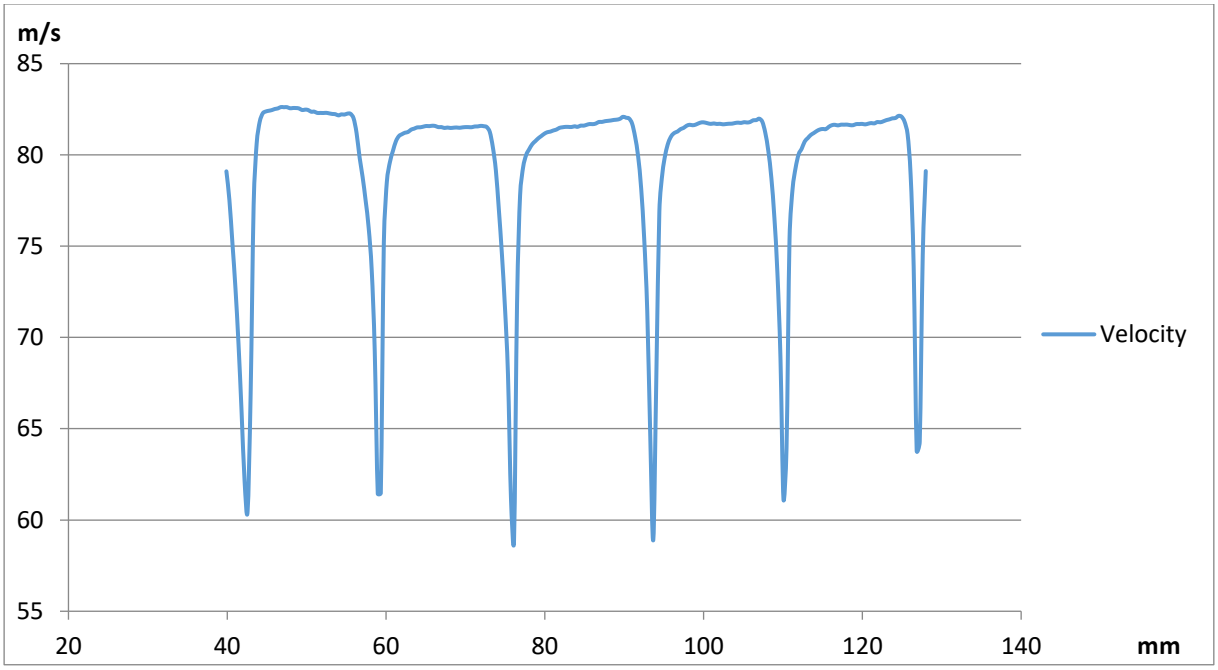

Figure 39 Velocity of the flow along the cascade at AoA = 5° and Ma = 0.2

Mach's number is calculated by dividing the velocity of the flow to the velocity of sound, the speed of sound is given by the equation:

$$v_{sound} = \sqrt{\frac{\gamma RT}{M}}\ [\text{m/s}] \tag{5.5}$$

Where, γ is the adiabatic constant, R is the universal gas constant, M is the molecular weight of the gas. For air is γ=1.4, R=8.314 J/mol.K, M= 28.95 gm/mol for dry air.

$$v_{sound} = 20.05\sqrt{T}\ [\text{m/s}] \tag{5.6}$$

For T = 4.5°C, the speed of sound is equal to $v_{sound} = 334$ [m/s], figure 40 shows the Mach's number profile for the cascade.

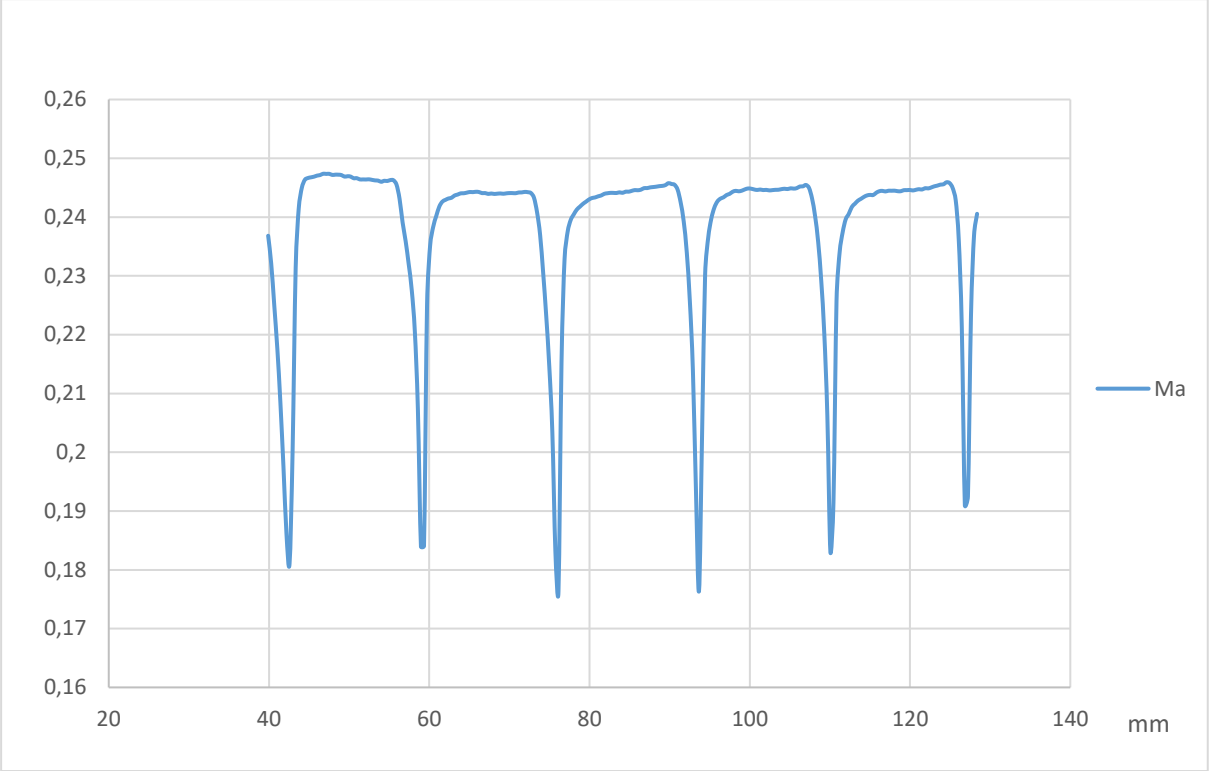

Figure 40 Mach's number for the flow along the cascade at AoA = 5° and Ma = 0.2

Second and third test:

In order to verify the uniformity of the flow field in the cascade, two additional tests were carried out at two different blade heights. One test was performed at AoA = 5°, Ma=0. 2 , and position of the sensors is at 16% of the blade height (Figure 38). The other test was performed at **AoA = 5°**, **Ma=0.2**, and position of the sensors is at 86% of the blade height (Figure 38).

Table 3 show the main parameters of the tests:

parameter	**unit**	2nd test	3rd test
t_in	**(°C)**	4.45	4.197
ps_in	**(Pa)**	97543	97436
pc_in	**(Pa)**	100334	100217
Ma_in	**(-)**	0.201	0.201
m_out	**(kg/s)**	1.019	1.017
AoA	**(°)**	5	5
Position of travers sensor	**(%)**	16	86

Table 4: main parameters of the second and third tests

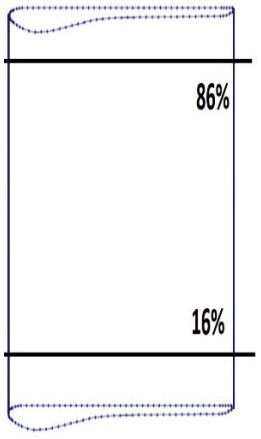

Figure 41: position of the sensors to the blade height

The results of first, second and third tests have revealed similar pressure profiles and the trends are compared in Figure 42.

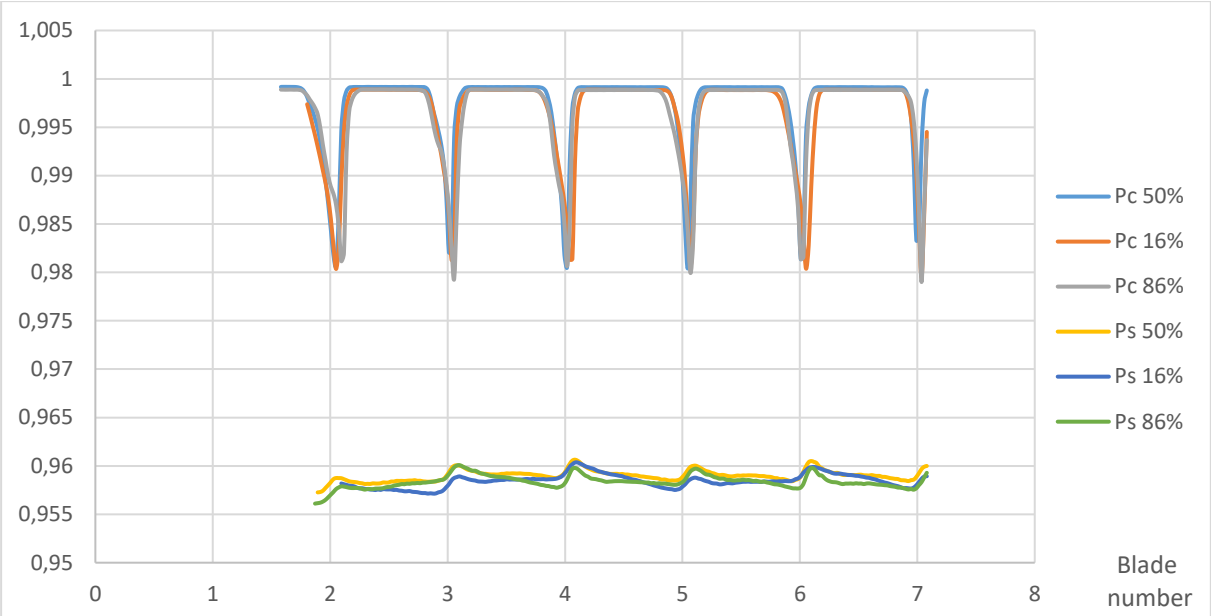

Figure 42 Cpc and Cps Pressure profiles comparison for the cascade at AoA = 5º and Ma = 0.2 at 16%, 50%, 86% of blades height

The comparison shows that along the height of the blade, the pressure profiles are alike. The total pressure loss downstream of the blade cascade in the inter-blade channels is approximately 0.1% and the total pressure loss in the wakes is around 2%. The static pressure trends at different blade heights are also in reasonable agreement.

Notice that the total pressure loss at the bottom and the top of the blade (yellow and green lines) is a bit higher than at the middle of the blade due to boundary layers effect of the walls, as shown in the figure 43:

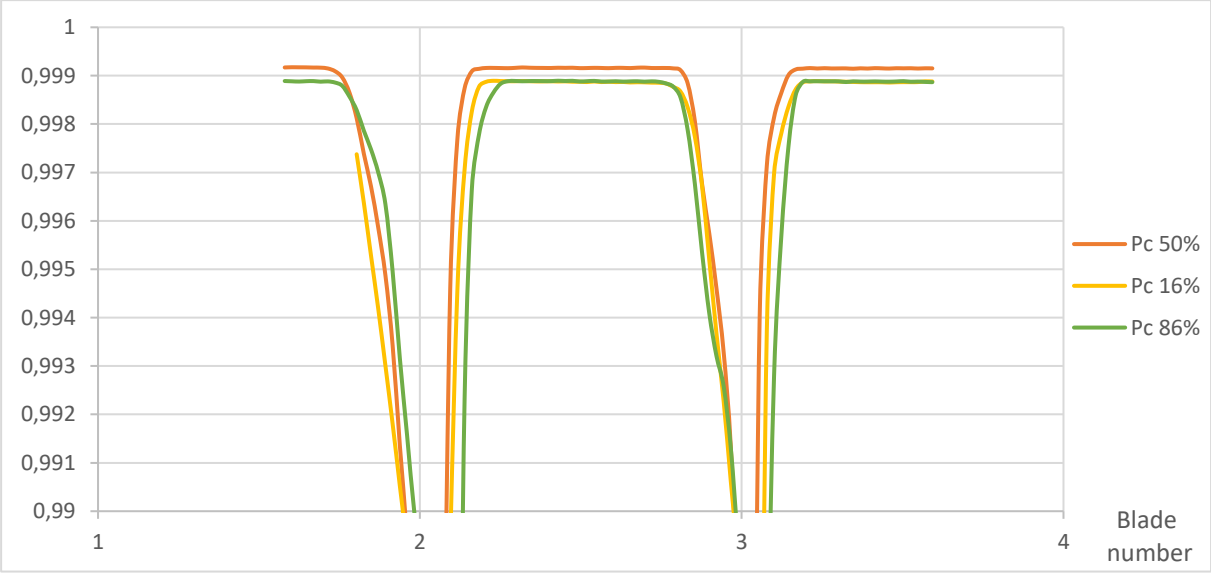

Figure 43 Effect of boundary layers of the walls on total pressure downstream the cascade

The dynamic pressure and the velocity profiles were also compared at different blade heights. The similarity of the trends without any major discrepancies is clear in Figures 44-46.

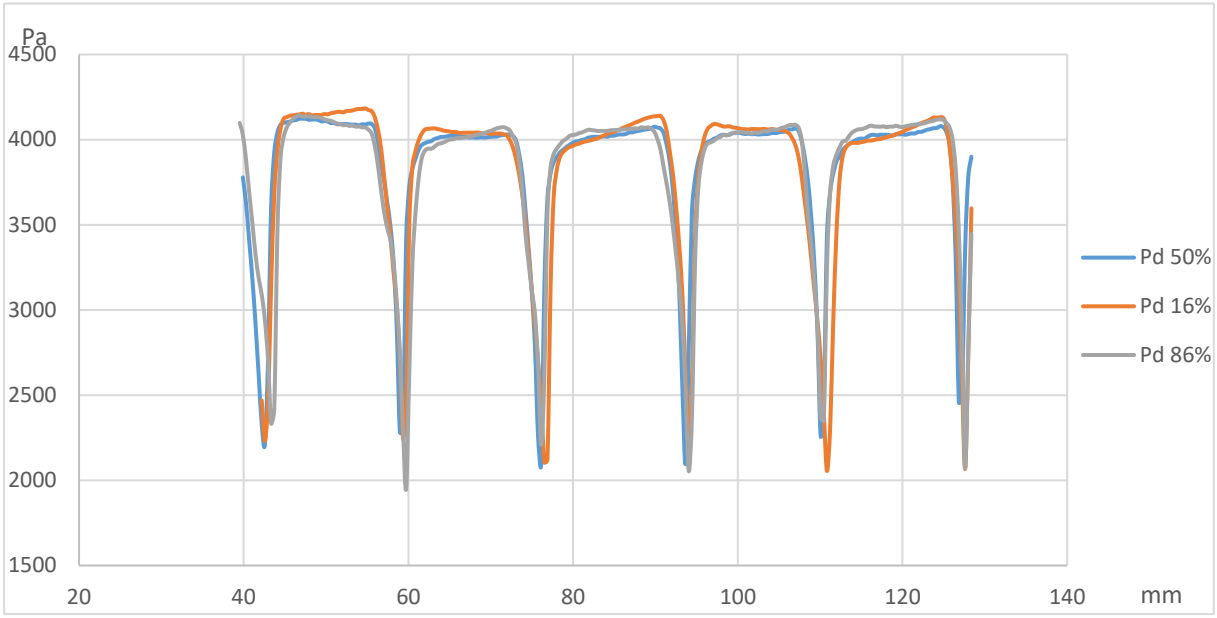

Figure 44 Dynamic Pressure profiles comparison for the cascade at AoA = 5º and Ma = 0.2 at 16%, 50%, 86% of blades height

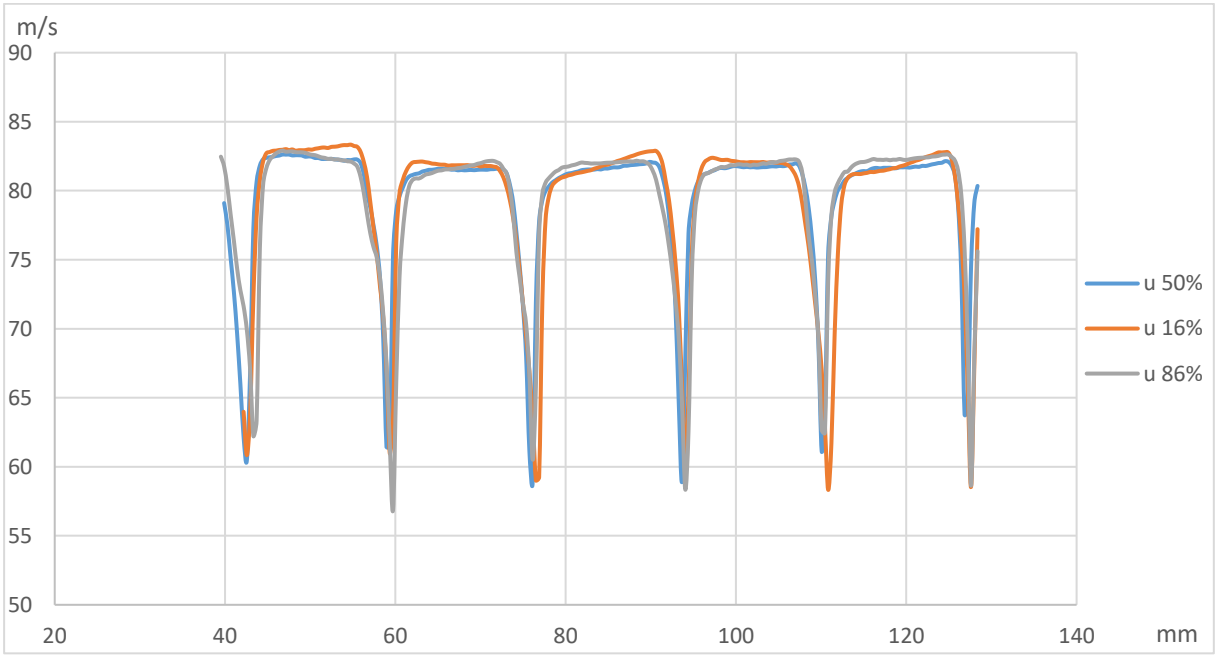

Figure 45 Velocity profiles comparison for the cascade at AoA = 5º and Ma = 0.2 at 16%, 50%, 86% of blades height

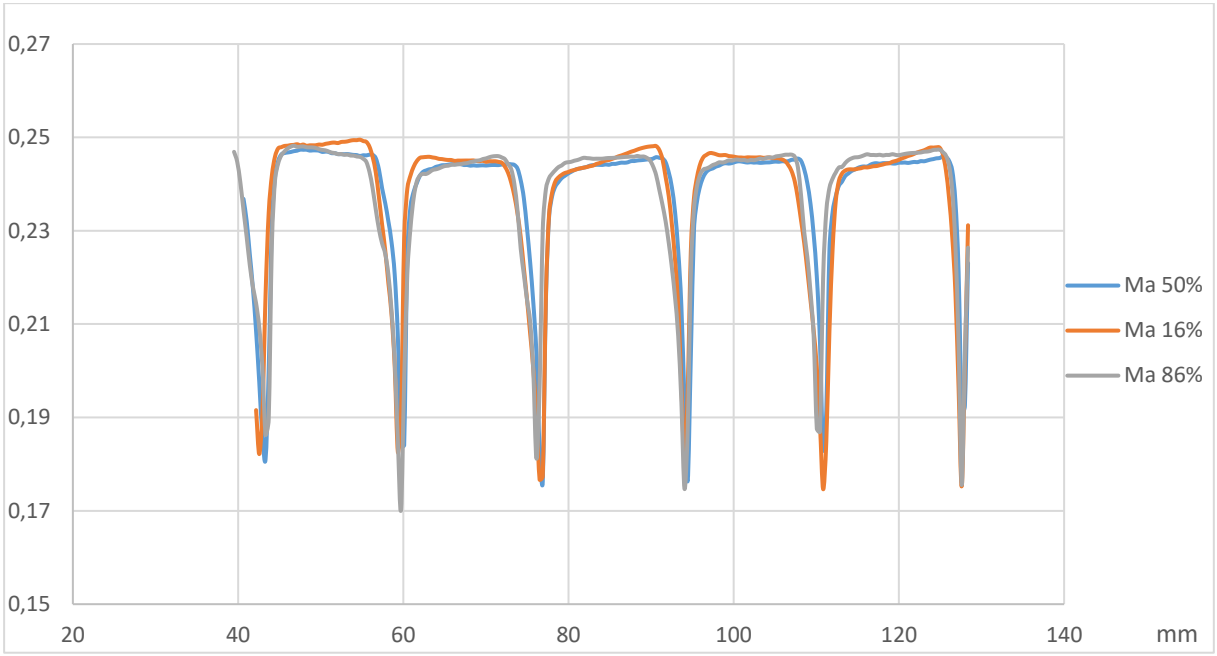

Figure 46 Mach's number for the flow along the cascade at AoA = 5° and Ma = 0.2 at 16%, 50%, 86% of blades height

Fourth test

To study the effect of the angle of attack and the effect of the inlet flow velocity on the blade cascade flow field, the fourth test was performed at **AoA = 0º**, **Ma=0.42** and position of sensor is at the middle of the blades. Data was given from previous test for the aim of comparison.

Table 4 shows the main parameters of the test:

t_in	**(°C)**	7.97
ps_in	**(Pa)**	88964.15
pc_in	**(Pa)**	100349.08
Ma_in	**(-)**	0.42
m_out	**(kg/s)**	1.55
AoA	**(°)**	0
Position of travers sensor	**(%)**	50

Table 5: main parameters of the fourth test

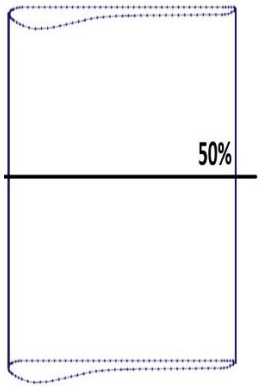

Figure 47: position of the sensors to the blade height

Results of the test are displayed in Figure 48

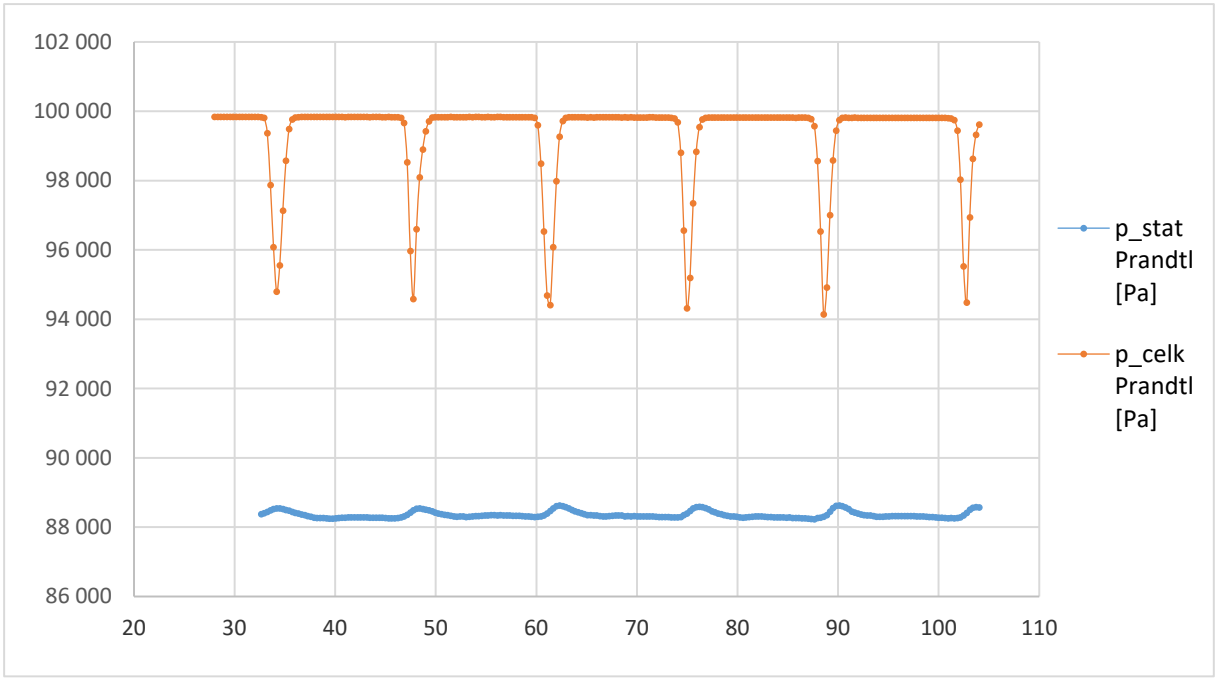

Figure 48 Pressure profile for the cascade at AoA = 0° and Ma = 0.42

It was observed that the qualitative character of flow in this test is similar to the previous tests, the total pressure downstream of the blades remains constant between the blades, the total pressure drop in the wakes is almost constant and the static pressure is nearly flat.

In order to quantify the effect of the angle of attack and the effect of the velocity, the pressure coefficients C_{pc} and C_{ps} were calculated according to equation (5.1) and the result is shown in figure 49.

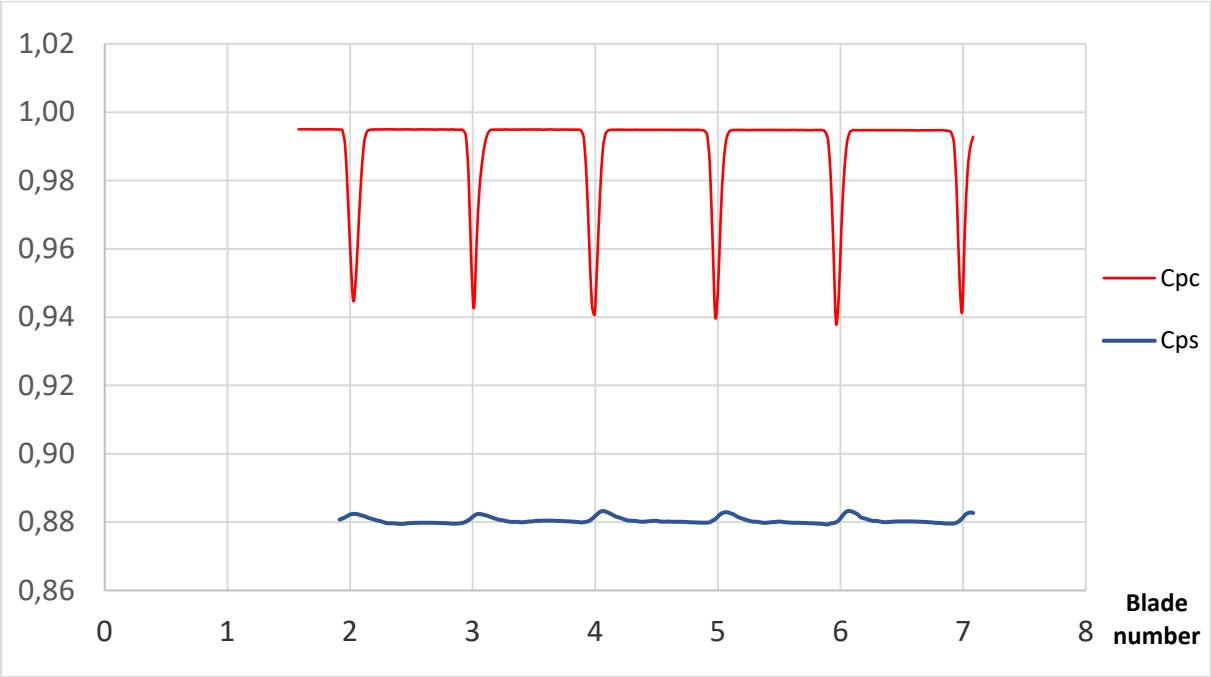

Figure 49 Pressure profile for the cascade at AoA = 0^o and Ma = 0.42 using Cpc and Cps

Notice the pressure loss in the wakes downstream the blades is bigger than the previous tests and is around 6% of the total pressure at the inlet of the cascade. It is because of the higher velocity of the flow. By comparing the forth test with the first test, where AoA=5^o and Ma= 0.2, two main effects can be observed (Fig.50):

1- **Effect of Angle of Attack (AoA):** The effect of different AoA is primarily observed in the vicinity of the wakes, for AoA=0^o the total pressure profile downstream of the cascade is approximately symmetric, while for AoA=5^o is not.

2- **Effect of Mach's number:** Increasing Mach's number leads to the increase of total pressure loss upstream and downstream the blade cascade and in the wakes. Also, the static pressure decreases, which leads to big increase of the dynamic pressure.

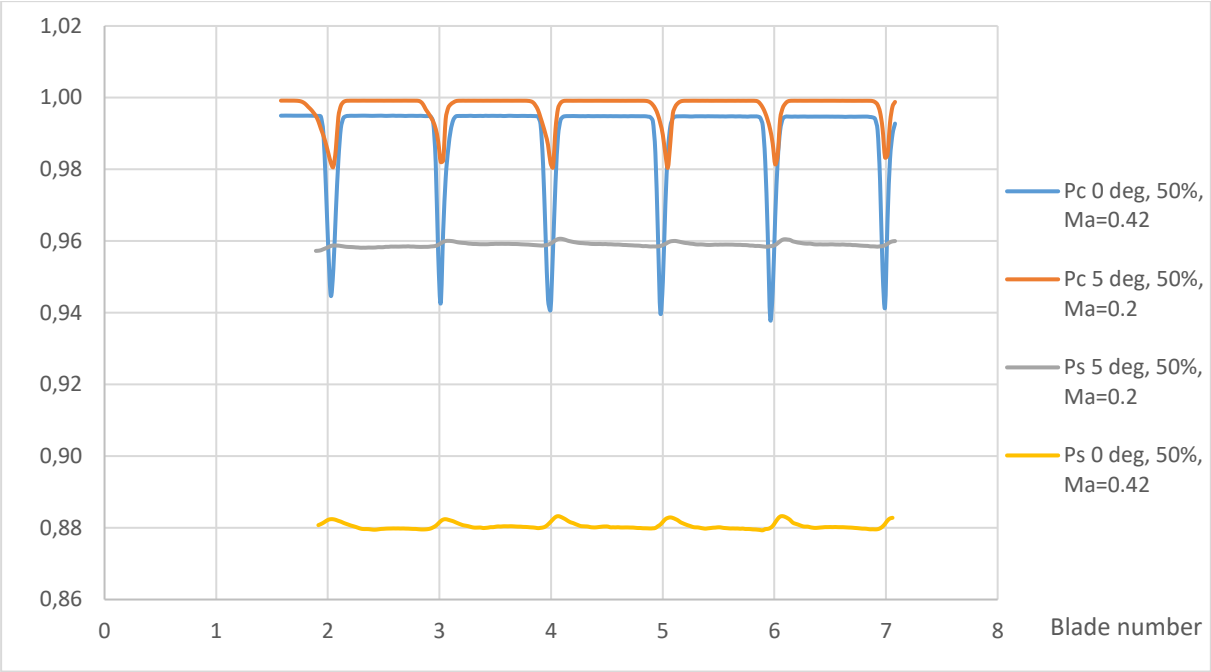

Figure 50 Cpc and Cps Pressure profiles comparison for the cascade at AoA = 0º and AoA = 5º at 50% blade height and different Mach numbers

The dynamic pressure for this case is calculated similarly to previous cases using equation (5.2), and the results are shown in figure 51. Notice the difference in dynamic pressures between Ma = 0.42 and Ma = 0.2 is caused by the decrease of the static pressure as shown in figure 50. The velocity of the flow for this case was not calculated as the simplistic assumption of the incompressible isothermal flow throughout the cascade was not applied.

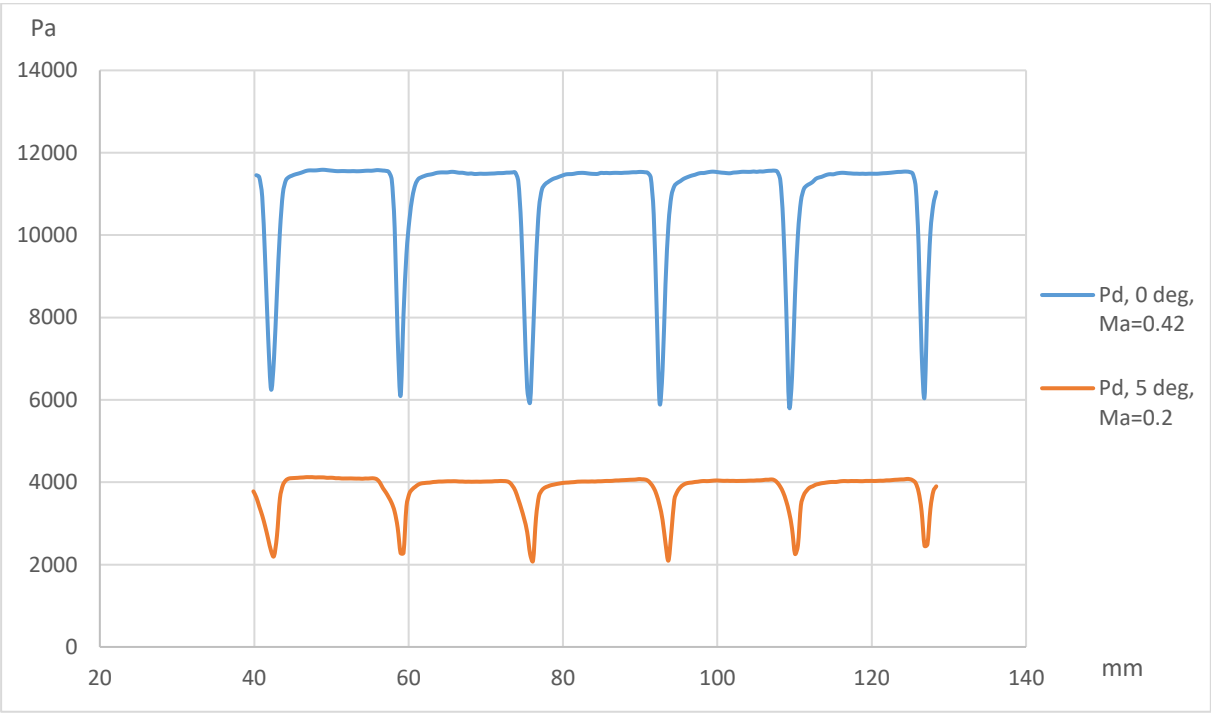

Figure 51 Dynamic pressure profile comparison for the cascade at AoA = 0º and AoA = 5º at 50% blade height

Flutter results:

An arbitrary motion of the blade profile will lead to an unsteady pressure distribution around the blade profile that in turn will result in an unsteady force on the profile. The work per oscillation cycle exerted by the fluid on the profile determines whether the flow has a stabilizing or a destabilizing character; in case of the fluid examining work on the structure the situation is referred to as unstable. In such case the work is per definition positive.

The flutter test was performed by oscillating the central four blades in the blade cascade by adapting the travelling wave mode approach. Only pure bending and torsion motions were considered, and no coupled bending-torsion motion has been investigated.

The main parameters for performed flutter test are:

- Amplitude of bending motion at blade root y= 0.7 mm
- Amplitude of torsion motion α_{grad} = 0.5 deg.
- AoA = 5°
- Mach number = 0.345
- K is reduced frequency, it is given by the equation

$$K = \frac{2\pi f b}{w} \tag{5.7}$$

- Frequency is f = 82.2 Hz
- Velocity of the flow w = 114.6 m/s
- $mdjoul\_y = 1000\pi b \frac{y}{b}$
- $mdjoul\_a = 1000\pi\alpha_{rad}$

Table 6 shows the values of the performed test, where h is the blade length, q is the dynamic pressure. Data was taken from previous test (not performed for the need of this thesis) due to the defect of one oscillator.

h[m]	b[m]	q[Pa]	w[m/s]	f [Hz]	K	y/b	α_{grad}	α_{rad}	mdjoul_y	mdjoul_a
0.0795	0.05	7919.9	114.6	82.2	0.22533	0.014	0.5	0,008726	2.19905	27.41395
Table 6: Parameters of flutter test										

As the imaginary part of aerodynamic forces and moments is related to system stability/instability (see section 4), figure 52 shows the imaginary part of aerodynamic lift force for each oscillating blade 1- 4 (blades 3-6 in the overall schematic of blade cascade in Fig. 25) at the bending vibration as a function of IBPA ranging from 0 to 360°. The corresponding aerodynamic work is depicted in Fig. 53 and is always negative, which means that in this test case the flow has no destabilizing effect on the vibrating cascade. By applying the equation (4.18), the aerodynamic work was calculated. The results are shown in Figure 53. As expected, the aerodynamic work caused by lift force is negative and blade cascade is stable.

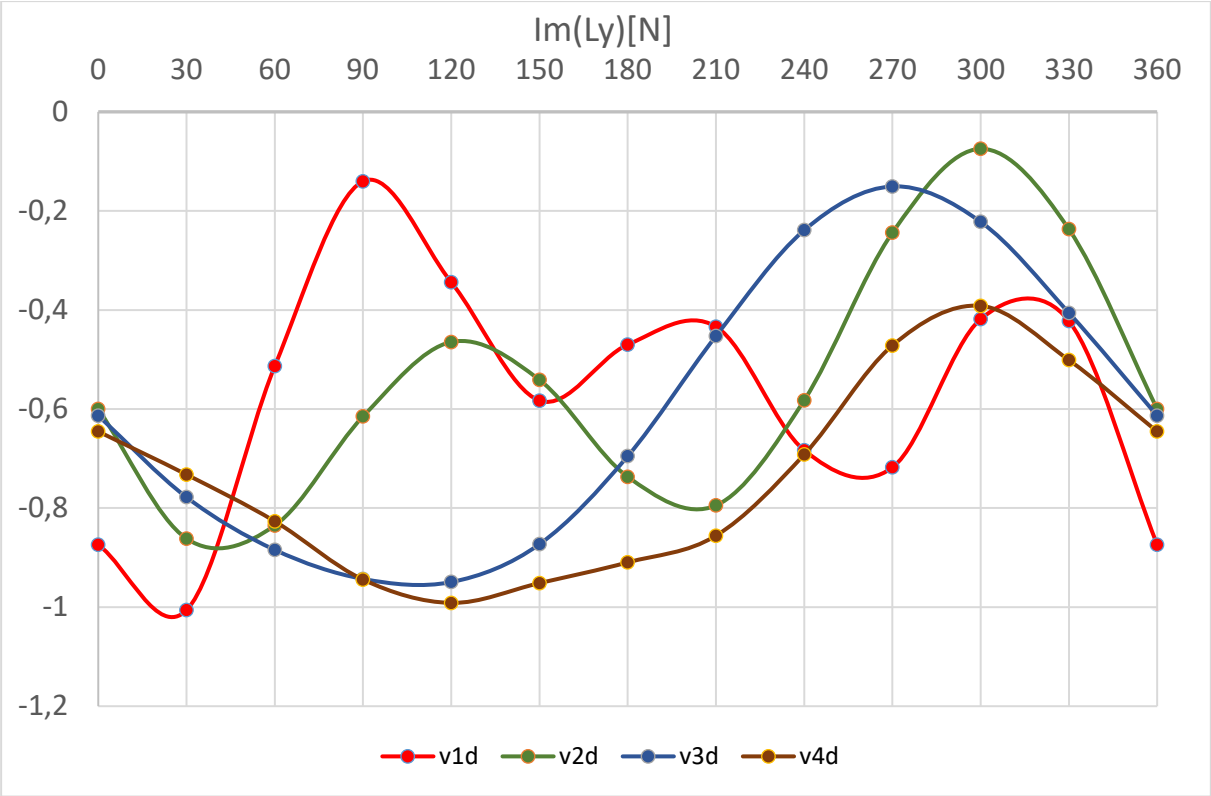

Figure 52 Imaginary part of aerodynamic lift force for blades 1- 4

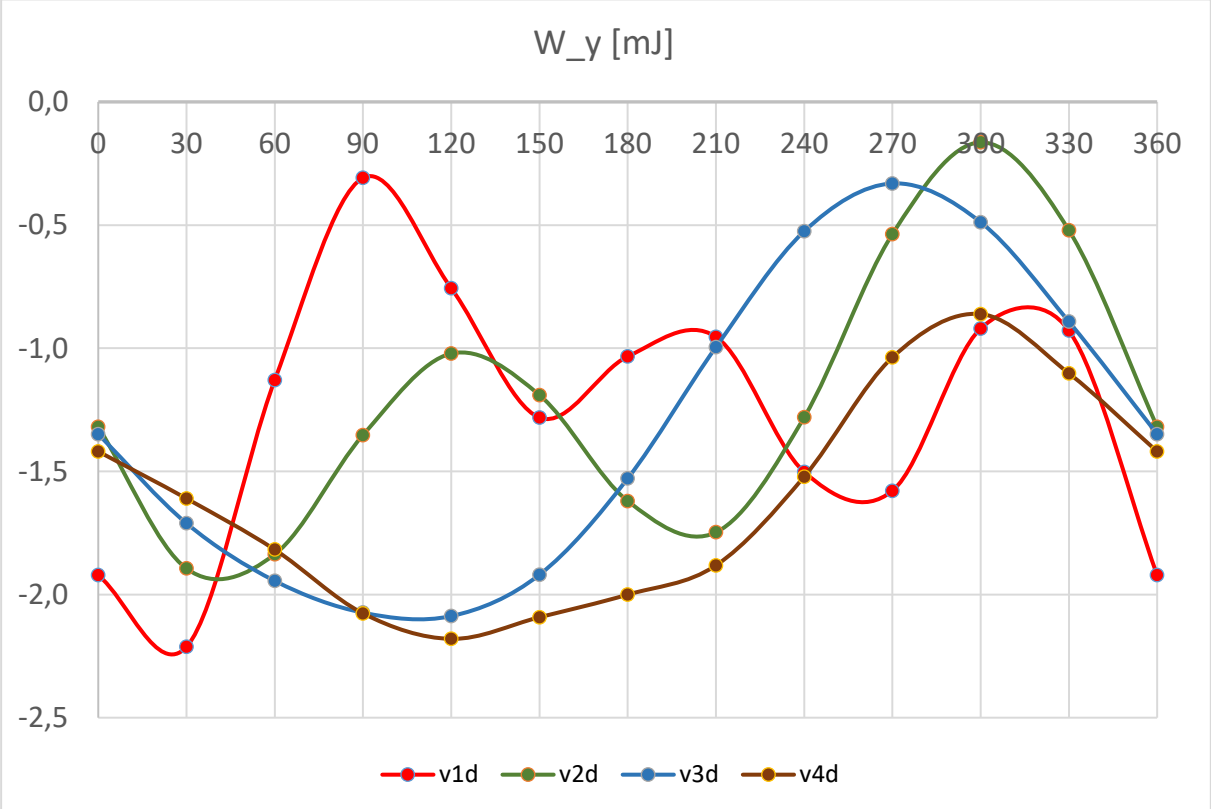

Figure 53 Aerodynamic work of lift force

Figure 54 shows the imaginary part of aerodynamic moment as a function of IBPA for torsion motion. For IBPA between 0° and 180°, the imaginary part of torsion moment has a positive value for all four blades, it means that the flow has a destabilizing effect on the cascade and the system is not stable. While for IBPA between 180° to 360° the value of imaginary part is negative, and the system is stable.

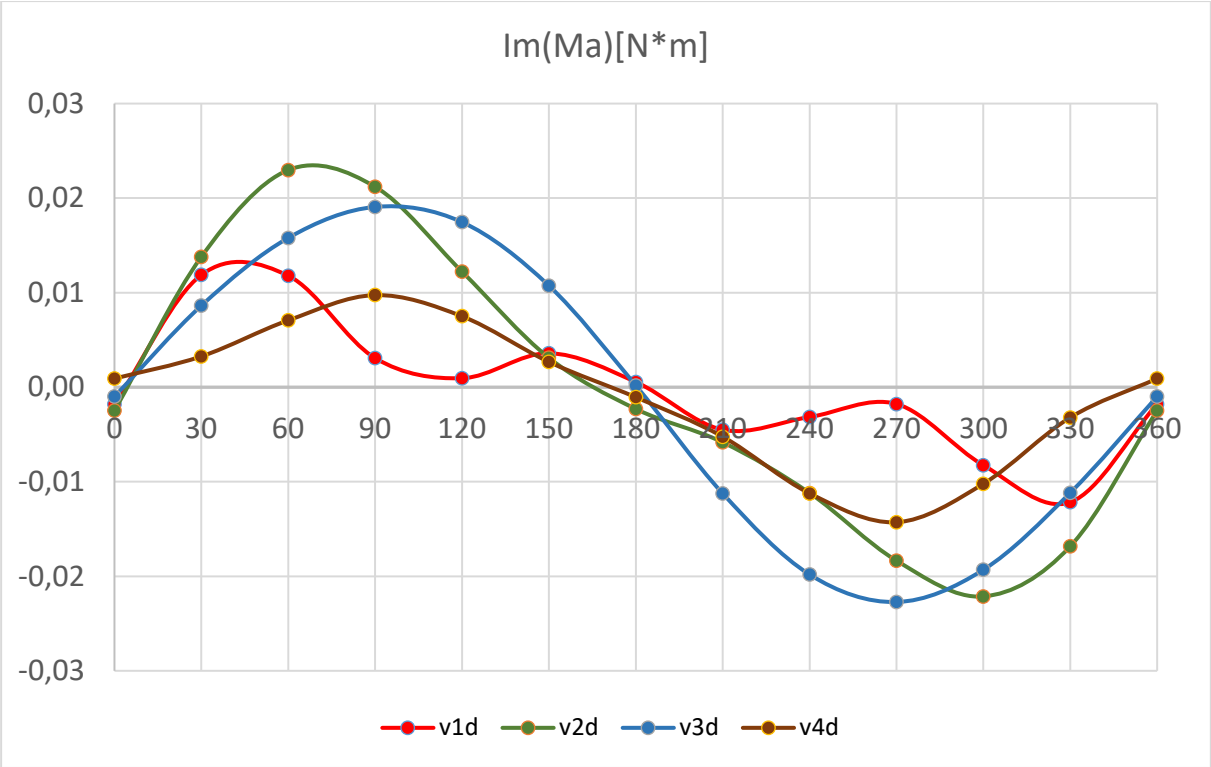

Figure 54 Imaginary torsion moment

The aerodynamic work of moment for torsion motion was also calculated and it is shown in figure 55. As it is a re-scale of imaginary part of aerodynamic moment (by using of equation (4.18)), the aerodynamic work of torsion moment has a positive value from IBPA between 0° and 180°, and negative value from 180° to 360°. Once again, this means a non-stable system for positive work and a stable system for the negative part of aerodynamic work.

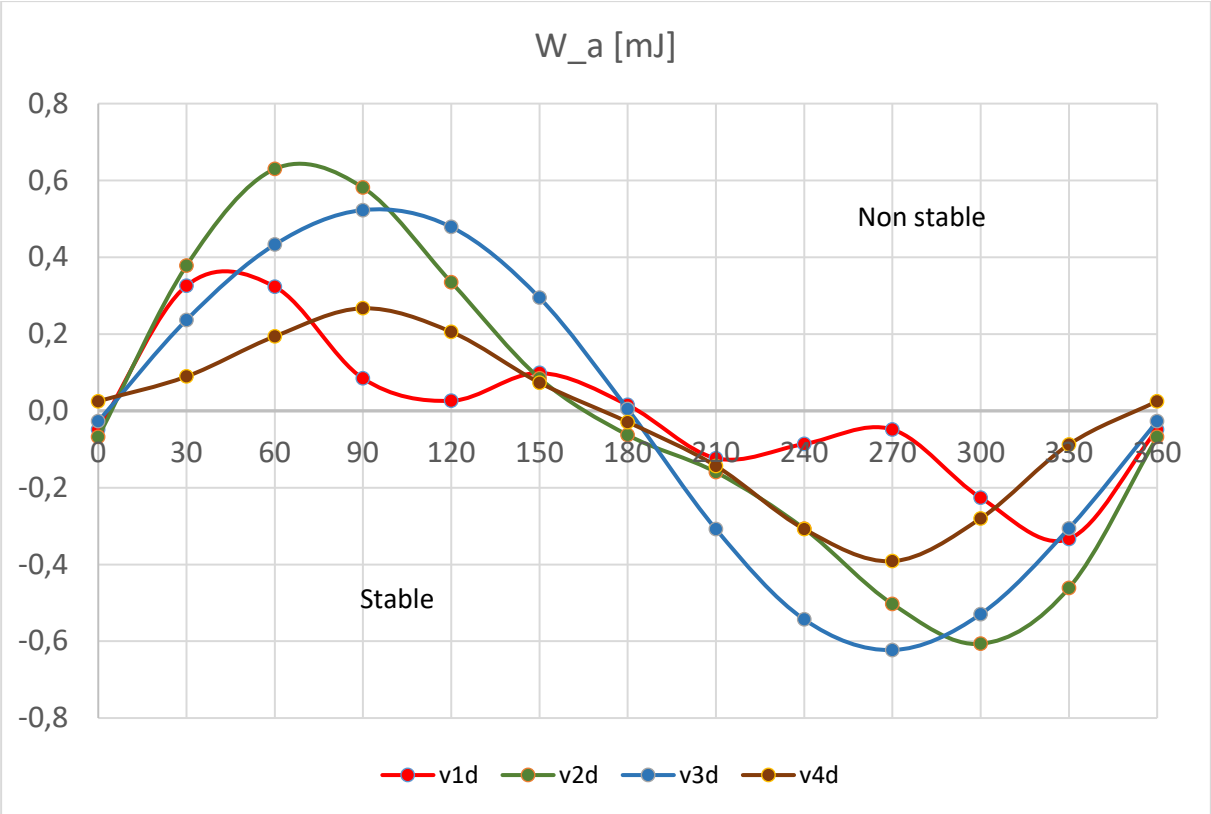

Figure 55 Aerodynamic work of moment

6 Conclusion

In this thesis, aerodynamic measurements of stationary and vibrating turbine blade cascade were performed and the associated testing methods were reviewed and described. Types of turbine blade cascade testing were commented and two main types, which are linear and annular, are detailed. Although annular blade cascades provide more accurate results in studying flutter, linear cascades are not so technically complex and a manageable level of flutter research is easily achievable at lower costs. A flutter phenomenon was studied, due to its negative effects that might lead to structural failure, and the methods of flutter measurement were discussed: free flutter testing and controlled flutter testing, which was further adopted in this work. Moreover, two methods of this controlled flutter testing (traveling wave mode and influence coefficient testing) were described.

Then, the experimental work of the thesis was performed on a test rig based at the University of West Bohemia. This test rig was described along with the main parameters for measurement. Several pressure profile measurements downstream of the stationary blade cascade were done for two different Angles of attack and at different blade heights: 16%, 50% 86%. These tests showed similar pressure profiles along the blade height, which means a reasonably uniformed flow in the blade cascade. Dynamic pressure, velocity and Mach number were also calculated for these tests. The effect of AoA and Mach number on the pressure profile trends downstream of the blade cascade was analyzed and it was shown that increasing of Mach number leads to an increase of pressure lost and increase of dynamic pressure. AoA has an effect on the symmetricity of pressure profile. Flutter testing using travelling wave mode approach has been carried out for pure bending and torsion motions of four flexibly mounted blades. Results showed that the imaginary parts of both lift force and torsion moment play the role of determining the stability of the system. Measurements revealed that the system was stable in the case of bending vibration, because the aerodynamic work was negative and had no destabilizing effect. While for torsion motion, the aerodynamic work had positive values for IBPA between 0^o to 180^o and negative values between 180^o to 360^o, which means that the flow had a destabilizing effect up to IBPA=180^o.

Annex: blade profile Geometry

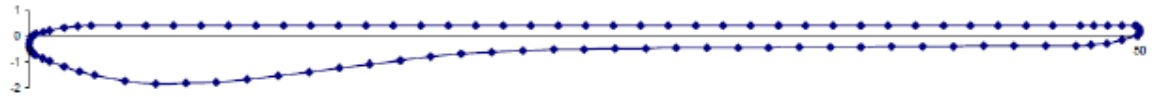

	x	y		x	y
1.	50,000	0,231	51.	0,104	-0,049
2.	49,965	0,317	52.	0,032	-0,168
3.	49,894	0,378	53.	0,000	-0,303
4.	49,803	0,400	54.	0,012	-0,442
5.	49,185	0,400	55.	0,067	-0,570
6.	48,566	0,400	56.	0,159	-0,675
7.	47,948	0,400	57.	0,279	-0,745
8.	47,329	0,400	58.	0,603	-0,867
9.	46,092	0,400	59.	0,930	-0,983
10.	44,855	0,400	60.	1,589	-1,192
11.	43,618	0,400	61.	2,257	-1,372
12.	42,380	0,400	62.	2,932	-1,525
13.	41,143	0,400	63.	4,298	-1,744
14.	39,906	0,400	64.	5,678	-1,845
15.	38,669	0,400	65.	7,061	-1,844
16.	37,432	0,400	66.	8,444	-1,798
17.	36,195	0,400	67.	9,823	-1,683
18.	34,957	0,400	68.	11,201	-1,550
19.	33,720	0,400	69.	12,576	-1,395
20.	32,483	0,400	70.	13,950	-1,233
21.	31,246	0,400	71.	15,326	-1,083
22.	30,009	0,400	72.	16,703	-0,943
23.	28,772	0,400	73.	18,081	-0,813
24.	27,534	0,400	74.	19,461	-0,711
25.	26,297	0,400	75.	20,843	-0,635
26.	25,060	0,400	76.	22,225	-0,579
27.	23,823	0,400	77.	23,609	-0,542
28.	22,586	0,400	78.	24,992	-0,519
29.	21,349	0,400	79.	26,376	-0,506
30.	20,111	0,400	80.	27,760	-0,487
31.	18,874	0,400	81.	29,144	-0,472
32.	17,637	0,400	82.	30,528	-0,473
33.	16,400	0,400	83.	31,911	-0,474
34.	15,163	0,400	84.	33,295	-0,465
35.	13,925	0,400	85.	34,679	-0,454
36.	12,688	0,400	86.	36,063	-0,444
37.	11,451	0,400	87.	37,447	-0,434
38.	10,214	0,400	88.	38,831	-0,424
39.	8,977	0,400	89.	40,215	-0,414
40.	7,740	0,400	90.	41,598	-0,404
41.	6,502	0,400	91.	42,982	-0,393
42.	5,265	0,400	92.	44,366	-0,381
43.	4,028	0,404	93.	45,750	-0,390
44.	2,791	0,396	94.	47,134	-0,396
45.	2,173	0,369	95.	47,825	-0,363
46.	1,557	0,309	96.	48,513	-0,294
47.	0,946	0,218	97.	49,193	-0,167
48.	0,642	0,160	98.	49,862	0,011
49.	0,340	0,094	99.	49,942	0,059
50.	0,211	0,041	100.	49,992	0,138

Tab.č. 4 Tabulka bodů profilu lopatky

References

1. NOWINSKI, M., PANOVSKY, J., Flutter Mechanisms in Low Pressure Turbine Blades, J. Eng. Gas Turbines Power 122(1), 1999, 82-88
2. SLAMA, V., RUDAS, B., IRA, J., MACALKA, A., ERET, P., TSYMBALYUK, V., CFD prediction of flutter of turbine blades and comparison with an experimental test case., 2018, MATEC Web of Conferences 168, 02005
3. TSYMBALYUK, V. A., Method of measuring transient aerodynamic forces and moments on a vibrating cascade, Strength of Materials (1996) 28: 150
4. VOGT, D., Experimental Investigation of Three-Dimensional Mechanisms in Low-Pressure Turbine Flutter, KTH, PhD thesis, 2005
5. FERRIA H., Contribution to numerical and experimental studies of flutter in space turbines : aerodynamic analysis of subsonic and supersonic flows in response to a prescribed vibratory mode of the structure, 2012, HAL
6. CITAVÝ, J., NOŽIČKA, J., *Lopatkové mříže.* Praha: ČVUT, 2003. ISBN 80-01-02653-1
7. SLAMA, V., RUDAS, B., IRA, J., MACALKA, A., ERET, P., TSYMBALYUK, V., PINELLI, L., VANTI, F., ARNONE, A., LO BALBO, A., Experimental and numerical study of controlled flutter testing in a linear turbine blade cascade, 2018, 20:98–107
8. Basic Principles of Turbomachines, https://nptel.ac.in/courses/112104117/#
9. VOGT, D., Experimental Research on Aeroelasticity, Royal Institute of Technology, Sweden, RTO-EN-AVT-2%